2019-12

UNDERWATER SHOCK MODELING

Hardman, Daniel J.

Monterey, CA; Naval Postgraduate School

NAVAL POSTGRADUATE SCHOOL

MONTEREY, CALIFORNIA

THESIS

UNDERWATER SHOCK MODELING

by

Daniel J. Hardman

December 2019

Thesis Advisor: Young W. Kwon
Second Reader: Jarema M. Didoszak

THIS PAGE INTENTIONALLY LEFT BLANK

REPORT DOCUMENTATION PAGE			Form Approved OMB No. 0704-0188

1. AGENCY USE ONLY *(Leave blank)*	2. REPORT DATE December 2019	3. REPORT TYPE AND DATES COVERED Master's thesis

4. TITLE AND SUBTITLE UNDERWATER SHOCK MODELING	5. FUNDING NUMBERS
6. AUTHOR(S) Daniel J. Hardman	
7. PERFORMING ORGANIZATION NAME(S) AND ADDRESS(ES) Naval Postgraduate School Monterey, CA 93943-5000	8. PERFORMING ORGANIZATION REPORT NUMBER
9. SPONSORING / MONITORING AGENCY NAME(S) AND ADDRESS(ES) N/A	10. SPONSORING / MONITORING AGENCY REPORT NUMBER

11. SUPPLEMENTARY NOTES The views expressed in this thesis are those of the author and do not reflect the official policy or position of the Department of Defense or the U.S. Government.

12a. DISTRIBUTION / AVAILABILITY STATEMENT Approved for public release. Distribution is unlimited.	12b. DISTRIBUTION CODE A

13. ABSTRACT (maximum 200 words)

Underwater explosions and their devastating effects are not new to the U.S. Navy; however, accurately modeling and scaling them for research and development is always an area of interest for anyone trying to protect the lives of the men and woman who serve on ships. Causing a large explosion for testing is not always easily conducted and accurately repeated. Frequency is also a common problem, without enough explosives readily available for testing purposes. Smaller models of underwater bubbles that cause the same type of shock wave as an explosive device can help determine how to prevent the damaging effects of underwater explosions more easily in more types of environments. The use of liquid nitrogen or dry ice in a sealed pressure vessel that is allowed to expand rapidly underwater is a great way of conducting safe and controlled experiments for testing. Once an accurate baseline was developed, the use of beams/plates with attached strain gauges were lowered into the water at different distances, angles, and depths from the explosion for testing. Then coatings and different pressure-relief devices were added to the structure to test how they would help a ship sustain less damage from an underwater explosion.

14. SUBJECT TERMS underwater explosions, modeling, simulating	15. NUMBER OF PAGES 87
	16. PRICE CODE

17. SECURITY CLASSIFICATION OF REPORT	18. SECURITY CLASSIFICATION OF THIS PAGE	19. SECURITY CLASSIFICATION OF ABSTRACT	20. LIMITATION OF ABSTRACT
Unclassified	Unclassified	Unclassified	UU

NSN 7540-01-280-5500 Standard Form 298 (Rev. 2-89) Prescribed by ANSI Std. 239-18

THIS PAGE INTENTIONALLY LEFT BLANK

Approved for public release. Distribution is unlimited.

UNDERWATER SHOCK MODELING

Daniel J. Hardman
Lieutenant, United States Navy
BE, SUNY Maritime College, 2013

Submitted in partial fulfillment of the
requirements for the degree of

MASTER OF SCIENCE IN MECHANICAL ENGINEERING

from the

NAVAL POSTGRADUATE SCHOOL
December 2019

Approved by: Young W. Kwon
Advisor

Jarema M. Didoszak
Second Reader

Garth V. Hobson
Chair, Department of Mechanical and Aerospace Engineering

THIS PAGE INTENTIONALLY LEFT BLANK

ABSTRACT

Underwater explosions and their devastating effects are not new to the U.S. Navy; however, accurately modeling and scaling them for research and development is always an area of interest for anyone trying to protect the lives of the men and woman who serve on ships. Causing a large explosion for testing is not always easily conducted and accurately repeated. Frequency is also a common problem, without enough explosives readily available for testing purposes. Smaller models of underwater bubbles that cause the same type of shock wave as an explosive device can help determine how to prevent the damaging effects of underwater explosions more easily in more types of environments. The use of liquid nitrogen or dry ice in a sealed pressure vessel that is allowed to expand rapidly underwater is a great way of conducting safe and controlled experiments for testing. Once an accurate baseline was developed, the use of beams/plates with attached strain gauges were lowered into the water at different distances, angles, and depths from the explosion for testing. Then coatings and different pressure-relief devices were added to the structure to test how they would help a ship sustain less damage from an underwater explosion.

THIS PAGE INTENTIONALLY LEFT BLANK

TABLE OF CONTENTS

THIS PAGE INTENTIONALLY LEFT BLANK

LIST OF FIGURES

THIS PAGE INTENTIONALLY LEFT BLANK

LIST OF TABLES

THIS PAGE INTENTIONALLY LEFT BLANK

LIST OF ACRONYMS AND ABBREVIATIONS

DoD	Department of Defense
FEA	Finite element analysis
LCS	Littoral combat ship
NPS	Naval Postgraduate School
PVC	Polyvinyl chloride
TNT	Trinitrotoluene
USN	United States Navy

THIS PAGE INTENTIONALLY LEFT BLANK

ACKNOWLEDGMENTS

I would like to thank my friends and family (in my eyes, one and the same) for their unwavering support. Without it, this thesis certainly would not have reached its culmination. I would like to thank Professor Wang for helping me think outside of the box and use resources from the entire campus and not just ones from the cold, dark engineering building. I also am grateful to Professor Bingham for his help filtering out my data and ensuring I was able to record the most accurate information. In addition, I would like to thank Professor Didoszak for his insight into naval architecture and reminders to never stray far from the roots of my knowledge and the things for which I am most passionate. Last but most certainly not least, I would like to thank my advisor, Professor Kwon, who, without any doubt in my mind, is the smartest man I have ever had the pleasure of knowing. Your ability to elevate my thinking to levels I never knew I could reach is truly inspiring. The Navy and anything you touch will surely benefit from your knowledge and passion.

THIS PAGE INTENTIONALLY LEFT BLANK

I. INTRODUCTION

The ability to move completely away from shock trials for Navy ships is not likely to occur in the near future. Each first ship of her class must undergo a full shock trial at sea. This is no small test. Its inherent complexity involves great expense, with possible damage to equipment and high risk to personnel.

With this in mind, this research attempts to determine whether the use of small-scale models can help the Navy slowly move away from full ship shock trials, and at the same time, learn and understand more about the damaging effects of underwater explosions.

The development of advanced computer modeling especially with Finite Element Analysis (FEA) has been making complex problems more easily solvable for years. However, it is unable to completely remove the need for a full ship shock trial, just like FEA still is unable to remove the need for tow tank experimentation and research in naval architecture during the research and development of a new ship hull [1], [2]. This experiment is the underwater shock trial equivalent to a tow tank in hull design. It allows anyone from a child with a new cardboard cutout design of the next battle ship to the graduate student working on his thesis or design project to try out their ideas. This simple theory and approach to testing is important to apply to many aspects of ship design and Department of Defense (DoD) research.

Not every idea will obtain the necessary funding in a competitive battle space. It is important to question how many ideas are thrown out that might possibly have provided the next upper hand advantage over an adversary just because of a lack of funding. If, whenever possible, every idea, theory, coating, and application, should be tested fully until failure and then tested again. Only then, should the best ideas be implemented and sent out to the fleet to keep sailors safe.

Near peer threats is a common term in the U.S. Navy (USN) used to describe adversaries that are not always necessarily near in terms of distance, but near in terms of technology or competition. There are several ways to stay ahead of the enemy, and the

DoD employs many of them right here at the Naval Postgraduate School (NPS). More funding is always one option, but with budgets and competing designs, it is not always effective or available. Time and resources are also needed to retain a competitive edge and are utilized effectively here at NPS, as many graduate-level students rotate through attempting to solve current real-world problems that they have personally faced in their career or expect to see the DoD facing in the years to come.

Underwater shock from explosions and the implosions that follow are of great threat to all surface ships, submarines, and infrastructure such as bridges and tunnels near fleet concentration areas [3]. Testing solutions to mitigate the effects of these explosions and implosions, rapidly and consistently is important in staying ahead of the competition [4].

The intention of this experiment was to use a large body of water and an improvised explosive-like device. It is explosive only in the fact that it produces rapidly expanding and collapsing gas bubbles and the corresponding pressure waves commonly associated with them. Explosions happen very rapidly, therefore, using something improvised would likely not obtain the same speed as an actual explosion. Using that same theory, the pressure of an actual explosion would not be the same as that produced by the improvised device. This difference in pressure does provide some advantages, mainly, it is safer for both personnel and equipment. The primary question, however, was if the improvised explosion was scalable. Could a model of both ship and torpedo, bridge and explosive, tunnel and mine, be comparable to a full-scale explosive device used to attack and damage them in both size, pressure, and rate of time? The answer is not as straightforward or as simple as yes or no. This research however has several advantages being smaller. It greatly increases the level of safety, lowers the level of complexity, and allows for consistent, frequent repeat testing.

II. EXPERIMENTAL SET UP

The large body of water used was not a tow tank but rather a pre-existing but unused structure on NPS's campus known as an anechoic water chamber. This tank, found in Watkins Hall Room (128), was built in the early 2000s. The chamber was dry, covered and not in use for approximately ten years. The chambers previous purpose was assisting research students in underwater impact loading. Refer to Figures 1–3 for chamber initial design. The chamber is built with redwood lining the walls and floor in ten-centimeter triangular strips attached to a redwood furring backing. Behind the furring, sand is placed for safe expansion and contraction. This entire tank is flush mounted in the floor of the building with a reinforced slab of concrete. The importance of these triangular wooden pieces lining the floors and walls is how they react to pressure and or sound waves. They help keep reverberation and wave propagation to a minimum. These wooden pieces should be viewed to underwater pressure waves as a black curtain over a mirror would be viewed to rays of visible light. The wooden pieces simulate an infinite amount of water to an underwater explosion.

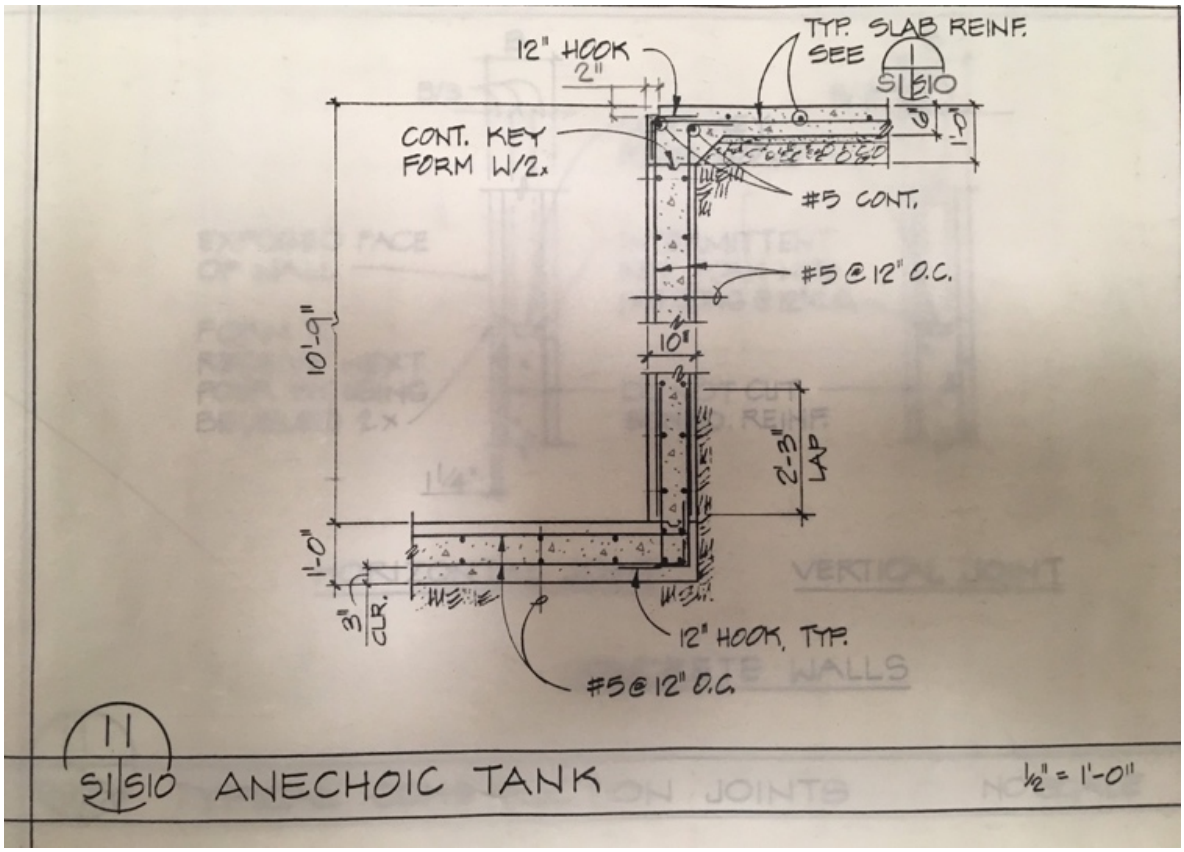

Figure 1. Anechoic tank initial design 1.

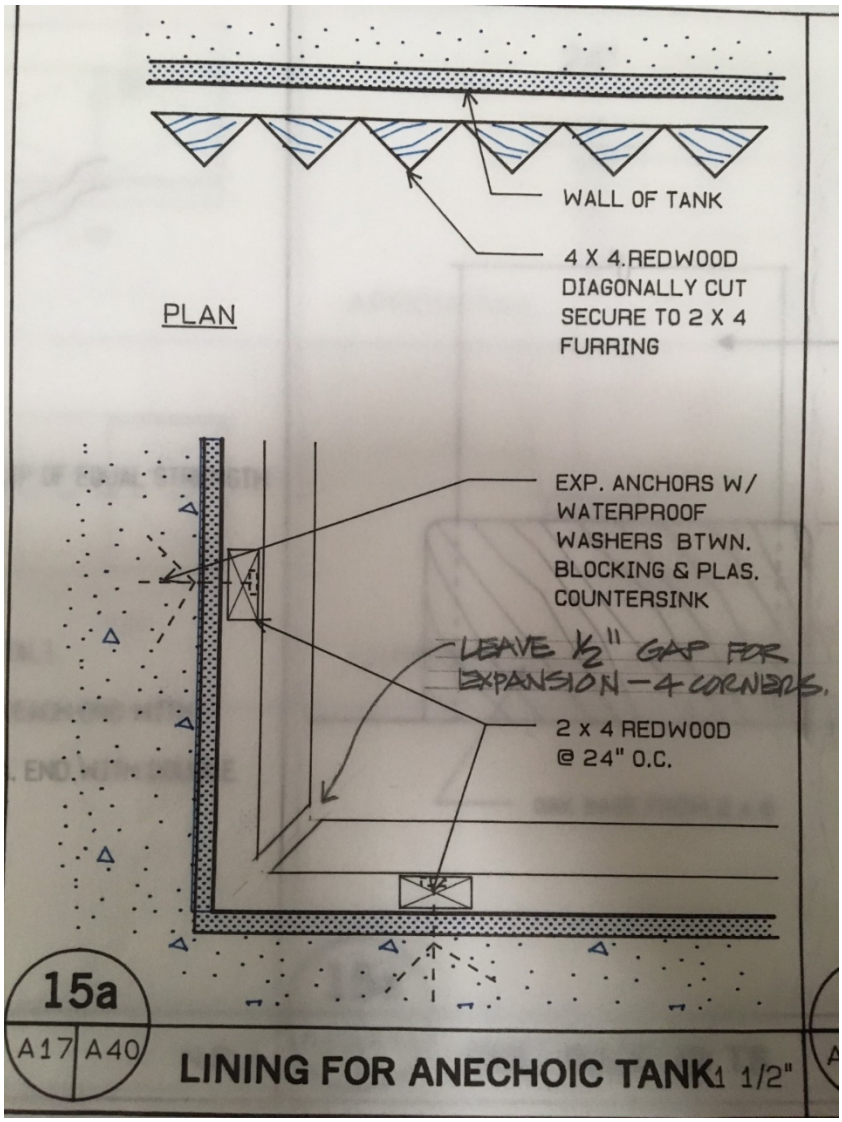

Figure 2. Anechoic tank initial design 2.

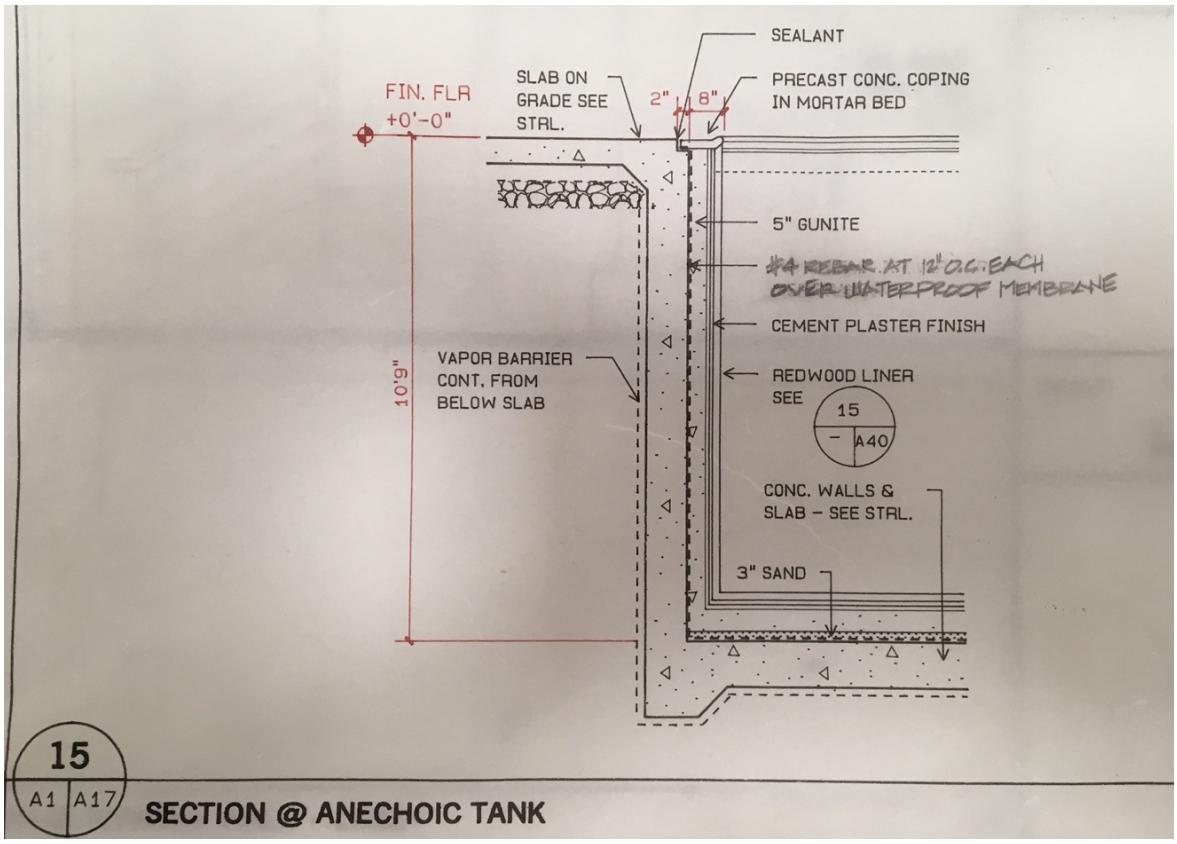

Figure 3. Anechoic tank initial design 3.

The water is pumped in and out of the tank via a standard household pool/spa pump. The pump is centrifugal in design, and utilizes polyvinyl chloride (PVC) piping with butterfly valves and three pool filters operating in parallel. The water is fresh and provided from the city of Monterey, California. The suction on the pump can be aligned to draw from the tank and discharge through the filters and back to the tank (recirculation) or the pump can also, with the aid of city water pressure, be aligned to fill the tank or drain it to the city sewer.

The tank can hold approximately 14498.13 liters of fresh water in its simple cubic design of 2.4 meters and it is open to the atmosphere at the top. This water can be chlorinated, or shocked for clarity. Sodium or Instant Ocean can be added to accurately represent the density of seawater. Sodium was not added to the tank for these experiments. All experiments were done in fresh water. A picture of the top of the tank while rigged and wired for testing can be seen in Figure 4.

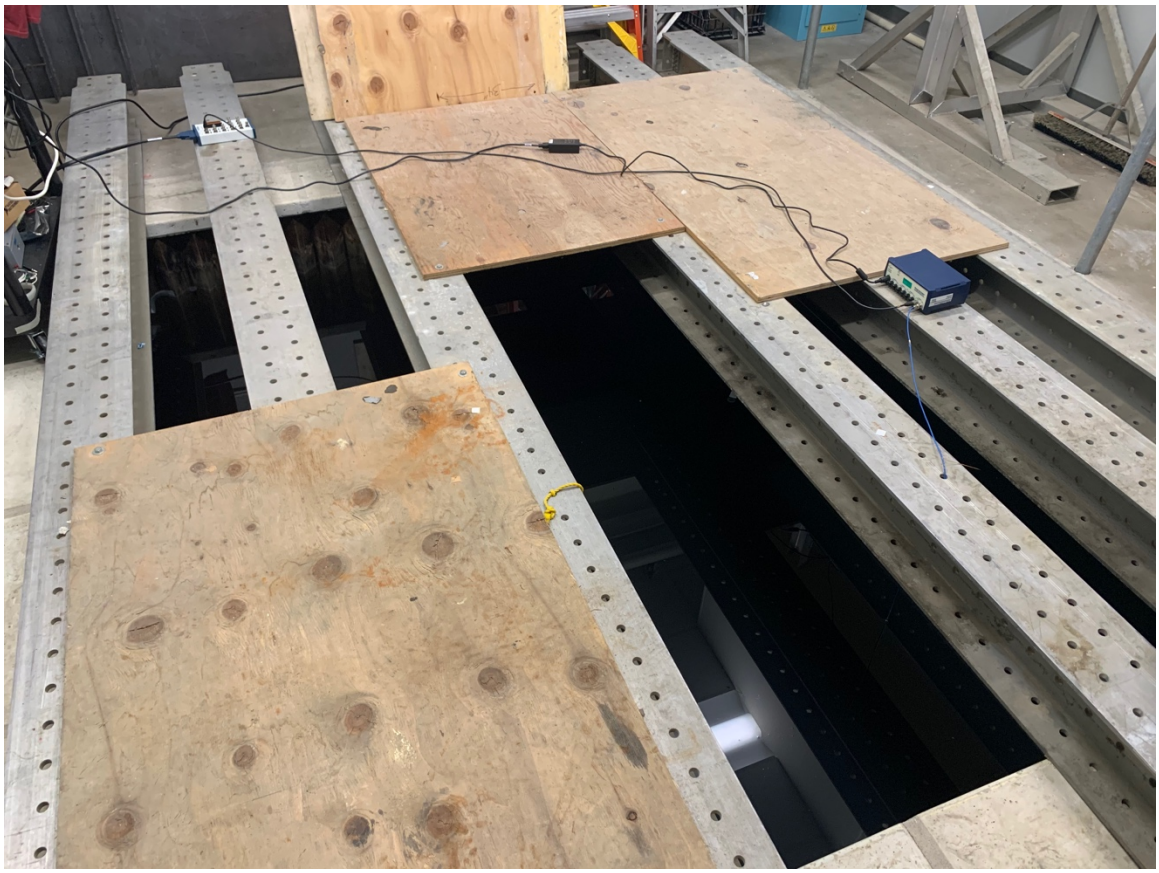

Figure 4. Anechoic chamber view from top during testing.

Several items were placed in the tank to conduct the experiment. The distances between the items, the walls, the floor and the surface were all accurately measured and recorded. Anchors were needed to tether these items in order for them to stay at certain distances and not float to the surface. These anchors were made of metal and are used to tether the pressure vessel and sensor in one place within the water column of the tank.

There were several types of pressure vessels used and compared in this experiment. All vessels were originally designed for holding liquids for personal drinking consumption. All were made of plastic and their designed cap was used to seal them and hold pressure. The volume of these pressure vessels varied and was noted to be of importance to the overall peak pressure of the tests. The volume of each pressure vessel was directly correlated to the amount of internal pressure force it could withstand before rupture and ultimate failure. The pressure vessel with a smaller volume was able to hold more internal

pressure force, which caused a higher peak pressure during the test. This higher pressure produced from a smaller pressure vessel is contradictory to what would be expected to that of an actual explosive device. Large explosive devices can hold more explosive causing a larger peak pressure.

A chemical reaction vice an explosion was chosen to produce pressure to be safely and easily controlled and conducted indoors at any time. There were two sources of pressure for the chosen pressure vessel: dry ice and liquid nitrogen. Dry ice was the primary medium as it was easier to handle, lower in cost, and more readily accessible. Dry ice was placed in each pressure vessel at a predetermined weight measured in grams. This weight, however, was not the deciding factor in how much pressure was produced. It was instead the overall volume and strength of the actual pressure vessel chosen that would determine peak pressure. However, the weight measured was kept constant in the effort to conduct an accurate and replicable experiment. Ten grams of dry ice was then mixed with 400ml of fresh water. The liquid nitrogen was also measured and held constant at 100ml of liquid nitrogen and no water was added to the pressure vessel.

The pressure vessel was intended to hold as much pressure as possible before rupture. Several methods were tested in order to accomplish this goal. Similar to how gases such as air compress in a combustion engine cylinder head, an air gap in the pressure vessel would also compress. Water is known to be an incompressible fluid, therefore adding it to the pressure vessel means only the elasticity of the vessel itself would expand before rupture. The air gap placed at the top of each pressure vessel before sealing it off and submerging it was used as a type of fuse. The expanding gasses would have to overcome the air gap along with the elasticity of the pressure vessel walls. Once this is fully compressed, the pressure vessel would start expanding until rupture.

Once the type of pressure vessel was selected, the pressure vessel's elasticity cannot be changed. Any slight difference in elasticity was noted to be manufacturing defects or slight inconsistencies in production. However, the amount of air gap left in the vessel can easily be changed by how much incompressible fluid (water) is added to the vessel for dry ice testing. For liquid nitrogen testing, this was not adjustable. The amount of air gap left in the top of the pressure vessel directly correlates to the length of delay in rupture. This

delay allows the pressure vessel to be anchored and set in the water tank at a specific depth in the water column and distance from the pressure sensor. It is important that the rupture be delayed to allow the water column to settle around the sensor in order to achieve the most accurate measurement.

The pressure sensor chosen is specifically designed for underwater blast and pressure analysis. The company chosen was PCB Piezotronics. PCB Piezotronics has a long history of working with underwater blast sensors for structural and environmental testing as well as for the DoD and the U.S. Navy (USN). The sensor series chosen was a 138A and is a non-resonating sensor made of tourmaline. Tourmaline is a naturally occurring piezoelectric material. It is preferred for underwater sensing when electrical charge is generated from the pressure [5]. The magnitude depends on the amount of hydrostatic pressure applied and the area over which the pressure acts. Tourmaline specifically has no center of charge symmetry, so it can respond to hydrostatic pressure only if electrodes are applied in the z-axis direction. This means that the placement of the sensors is critical in order to ensure accurate pressure measurements. Tourmaline also requires only a short period of time before it equalizes with the surrounding pressure of the water column in which it is placed.

The supplied Tygon tube is filled with silicon oil surrounding the tourmaline and helps to minimize early reflections in pressure inside the water column. The sensor sensitivity is .0145 to .73 mV/kPa and has a pressure sensitivity of 0kPa to 6900kPa. The pressure sensor equation of linearity can be seen below.

$$\frac{Output - MilliVolts(\,mV)}{Input - PSI} = \frac{1000(\,mV)}{200(\,PSI)}$$

The pressure sensor was carefully mounted vertically in the water column and tethered to the floor of the tank with monofilament and a small anchor. The waterproof cable is ten feet long and has an installed high shock version of a standard 10–32 plug. This cable is epoxy and O-ring sealed inside the connector and has two layers of shrink wrapping on the tube. The waterproof cable is also securely mounted to an aluminum I-beam running

across the top of the tank. This keeps slight tension on the pressure sensor making sure that it remains in place during testing.

The waterproof cable is then attached to a Platinum Stock Products four channel, line powered, signal conditioner. This signal conditioner is necessary to receive data from the pressure sensor using pre-purchased NPS data-acquiring equipment that will be discussed later in further detail. The signal conditioner uses standard Baby Neill Constant (BNC) connectors and has room for expansion of up to four channels for a total of four pressure sensors.

The signal conditioner is wired via a standard BNC connector cable to a National Instruments BNC-2110 noise rejecting, shielded BNC connector block. This block is then wired via a National Instruments SHC68-68-EP, 68-D type to 68 VHDCI offset shielded cable. This is wired directly into a National Instruments PXIe-6358 X series multifunction Data Acquisition (DAQ) card that is installed in a National Instruments PXIe-1071 computer with a Windows 7 operating system.

The PXIe-1071 computer was set up using maximum sampling rates in order to capture all data during the rapid expansion of the pressure vessel. The data was later able to be filtered out in MATLAB. The settings used were 400,000 samples to be read continuously every second and at a rate of 300,000Hz.

The sensor is accurate enough to detect vibrations produced from speaking voices in the same room as the tank. This sometimes causes noise to be detected that must be filtered out prior to analysis. Since this is a low-pressure test compared to what the sensor is capable of measuring, the noise threshold is close to the testing pressure.

III. DRY ICE AND LIQUID NITROGEN TESTING

When using either dry ice or liquid nitrogen the first step was to test for a constant pressure. It was possible to produce the same peak pressure repeatedly over several different tests. The maximum pressure obtained for dry ice testing was 20.479Pa. This Pressure was produced using 10 grams of dry ice and 300 milliliters of water in pressure vessel (1), as seen in Figure 5. Comparatively, the maximum pressure obtained for liquid nitrogen testing was 11.5Pa in pressure vessel (1), as seen in Figure 5. For liquid nitrogen and dry ice testing the pressure vessel was placed 1.2m from the bottom of the tank and at varying horizontal distances. The maximum pressures for both were obtained at the minimum distance of 0m. At a distance of 0m the sensor is touching the pressure vessel before the explosion. The pressure vessel was centered in the tank while the sensor was placed off to the side of pressure vessel closer to the wall of the tank. Several tests were conducted in this manner. Average pressures for each distance were obtained and can be seen in Table 1.

Figure 5. Pressure vessel 1 (maximum internal volume 400ml).

After average peak pressures were obtained, the next step was to test for a Po curve. A Po curve is made by plotting the measurement of max pressure vs distance from an explosion. Industry standard for this test is to use multiple sensors. Though this will be possible for future work and future thesis students, it was not possible for this experiment. In order to obtain the curve shown in Figures 6 and 8, constant pressure tests were performed at distances of 0m to 2.5m at .6m intervals. Three tests were performed at each distance and then averaged together to produce the curve shown in Figures 6 and 8. The pressure vessel and the sensor were both placed equal distances from the surrounding walls in the tank and with the center of the tank halfway between them.

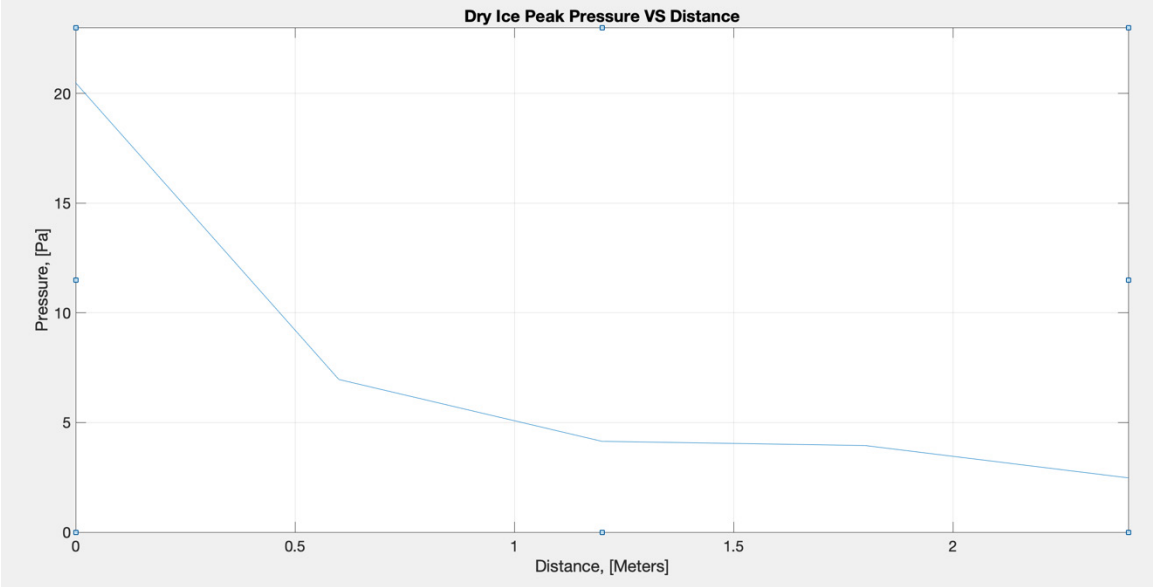

Figure 6. Dry ice peak pressure versus distance.

The raw dry ice data that was obtained from testing needed to be filtered before accurate analysis could be conducted. The amount of noise present from the sensor during testing was the reason for this filtering being required. Raw dry ice data before filtering can be seen in Figure 7. The filtering was conducted in MATLAB. This command can be seen in the Appendix B.

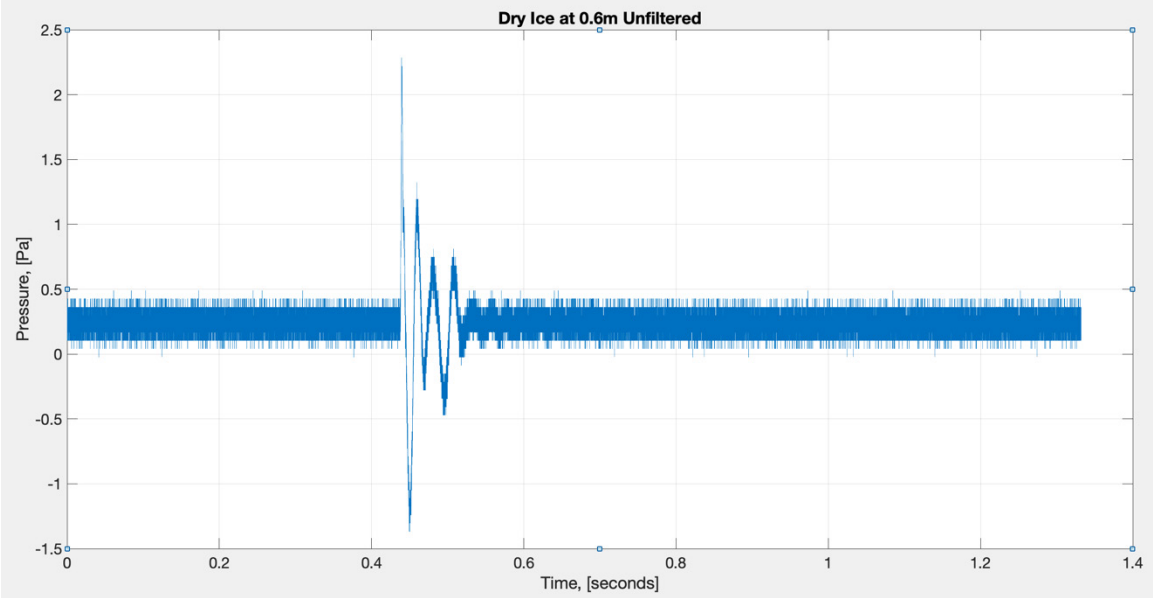

Figure 7. Dry ice at 0.6m unfiltered.

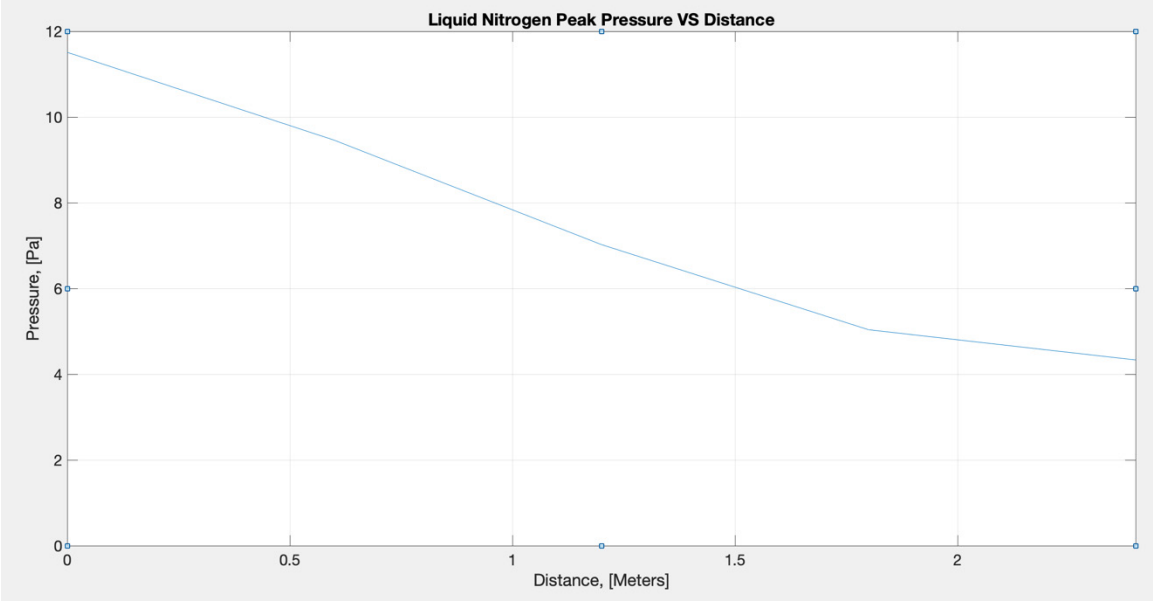

Figure 8. Liquid nitrogen peak pressure versus distance.

The liquid nitrogen data that was obtained was much cleaner in regards to noise then the dry ice data. Liquid nitrogen data unfiltered can be seen in Figure 9. Though the data did not need to be filtered to the same level as the dry ice data for proper analysis, a filter and filtering code were still applied in MATLAB and can be seen in Appendix C.

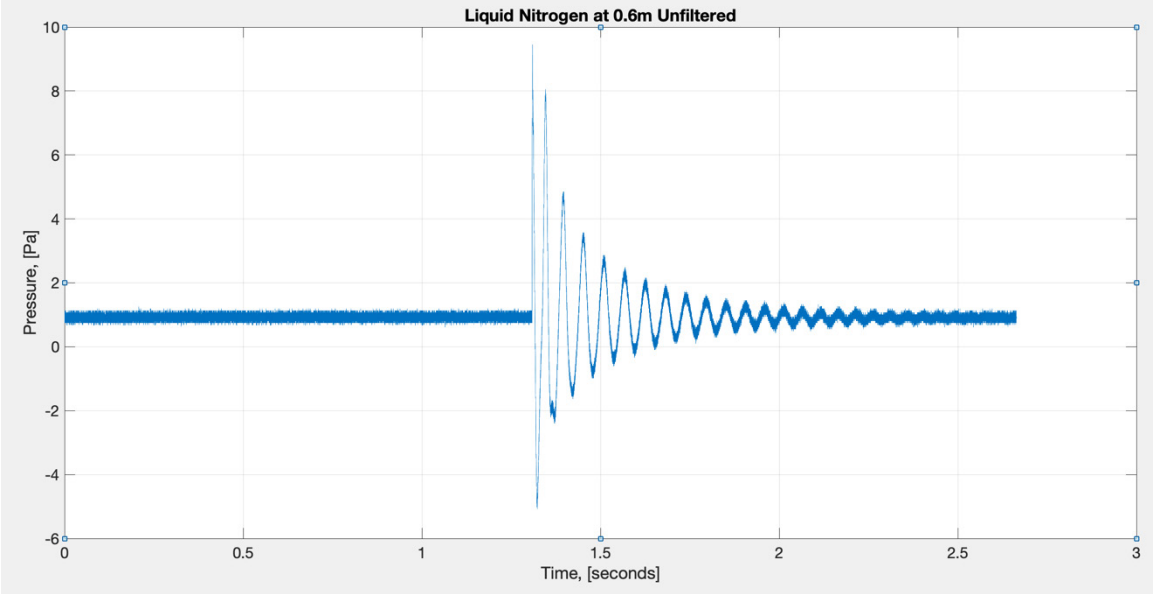

Figure 9. Liquid nitrogen at 0.6m unfiltered.

After peak pressure was constantly tested and achieved the next test was to make sure that the time in which the peak pressure was achieved was able to be replicated. This was done by calculating the time taken to reach the first initial peak and the rate or slope of the line in which the pressure arrived. This was then conducted at all distances and can be viewed in Table1. This is a slope equation of a line:

$$m = \frac{Rise}{Run} = \frac{Y_2 - Y_1}{X_1 - X_2} = \frac{Pressure_2(Pa) - Pressure_1(Pa)}{Time_2 - Time_1}$$

A. DRY ICE

Dry ice testing occasionally produced results that were just noise or did not provide much useful data. There are a few possibilities for this error. One possibility is the water inside of the pressure vessel expanded in a different way or at a different rate then other previous tests. Another possibility is the air gap at the top of the pressure vessel was measured incorrectly. The expanding gasses caused by the dry ice could have leaked through the cap on the pressure vessel. Manufacturing defects or slight inconstancies from the factory that made the pressure vessel could also have been a factor. These inconclusive tests and their corresponding graphs can be seen in Figures 18–19 and Figures 28–29.

Dry ice at 0m would occasionally cause a pressure that would move the sensor with the pressure vessel. This result can be seen in Figures 10–11 and Figures 20–21. These tests were not used for analysis. They do, however, show how the wave propagates through the water column.

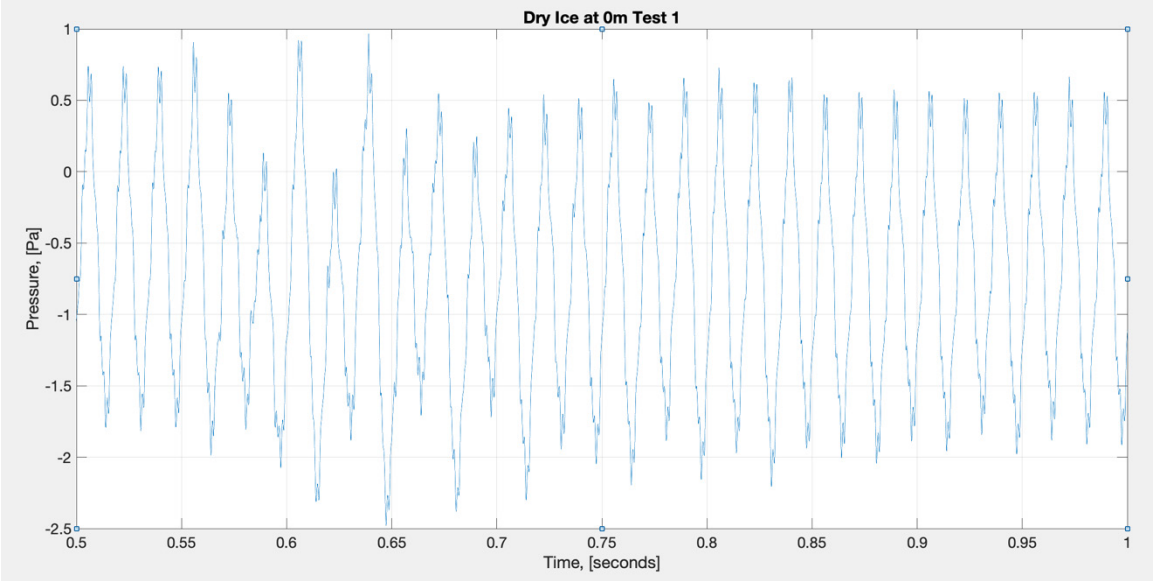

Figure 10. Dry ice 0m Test 1 zoomed.

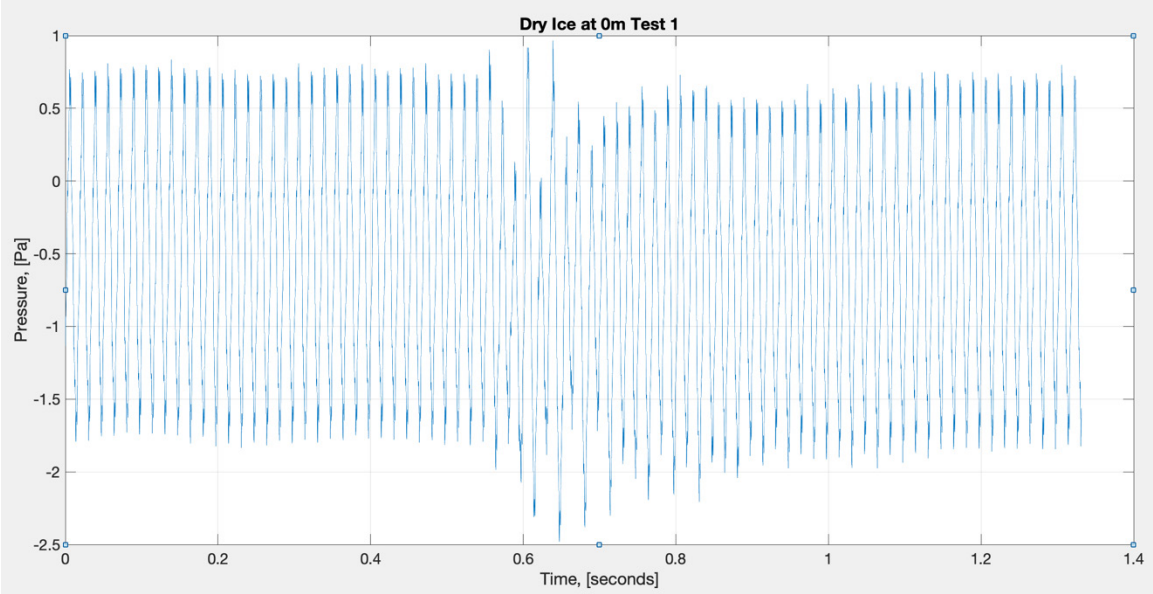

Figure 11. Dry ice at 0m test 1.

A dry ice pressure vessel at the closest range to the sensor 0m produced the highest peak pressure. The graph of this test can be seen in Figures 12 and 13.

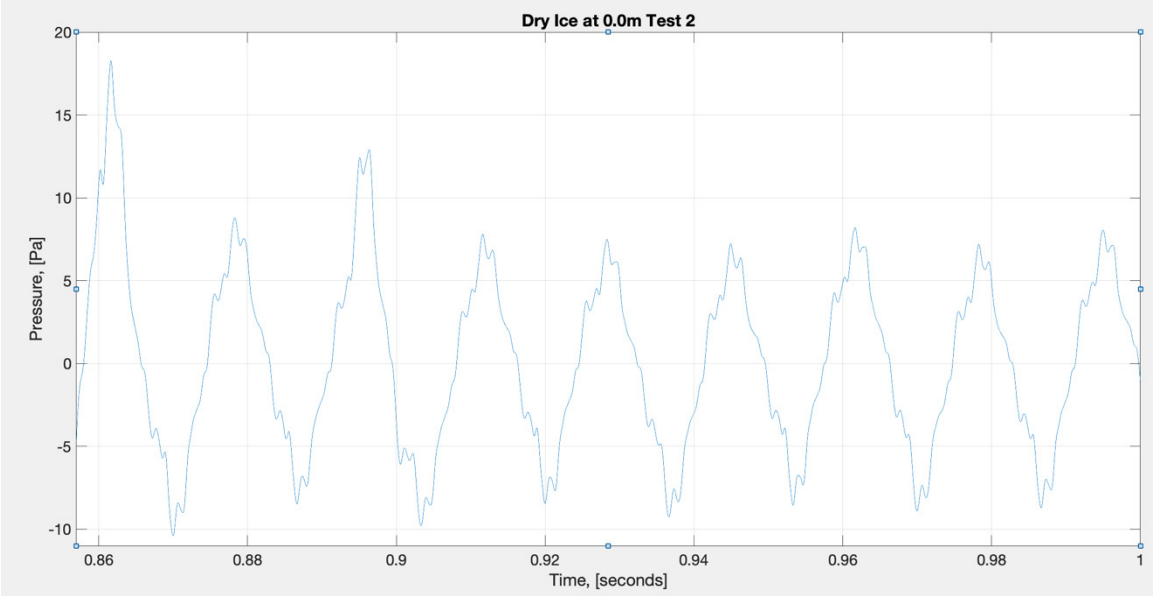

Figure 12. Dry ice at 0m test 2 zoomed.

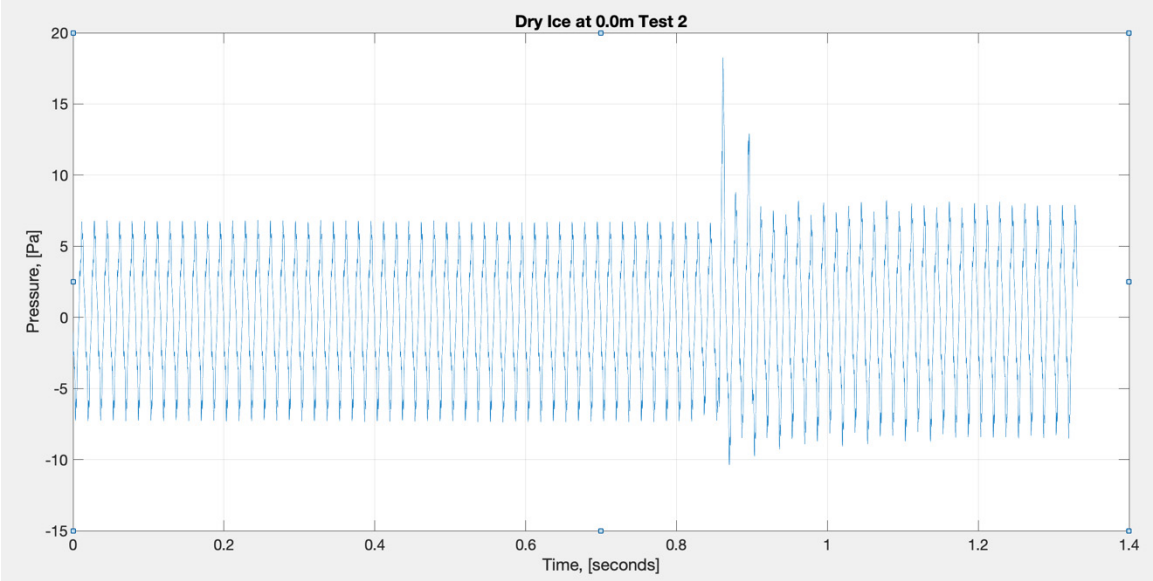

Figure 13. Dry ice at 0m test 2.

Certain dry ice tests had pulsations in pressure in the first peak. These pulsations were originally thought to be noise but upon further analysis and filtering were persistent and clearly visible, as seen in Figure 14,22,24,25,27,30,32. A few theories as to what might have caused these pulsations in pressure are addressed. One theory is the pressure vessel did not rupture cleanly along one seem. Another theory is that the pressure vessel cap could have leaked, allowing gas to relieve pressure before total rupture. The last likely theory for this could also be from the shock wave and the vacuum that follows due to the large displacement of water caused by the bubble [6].

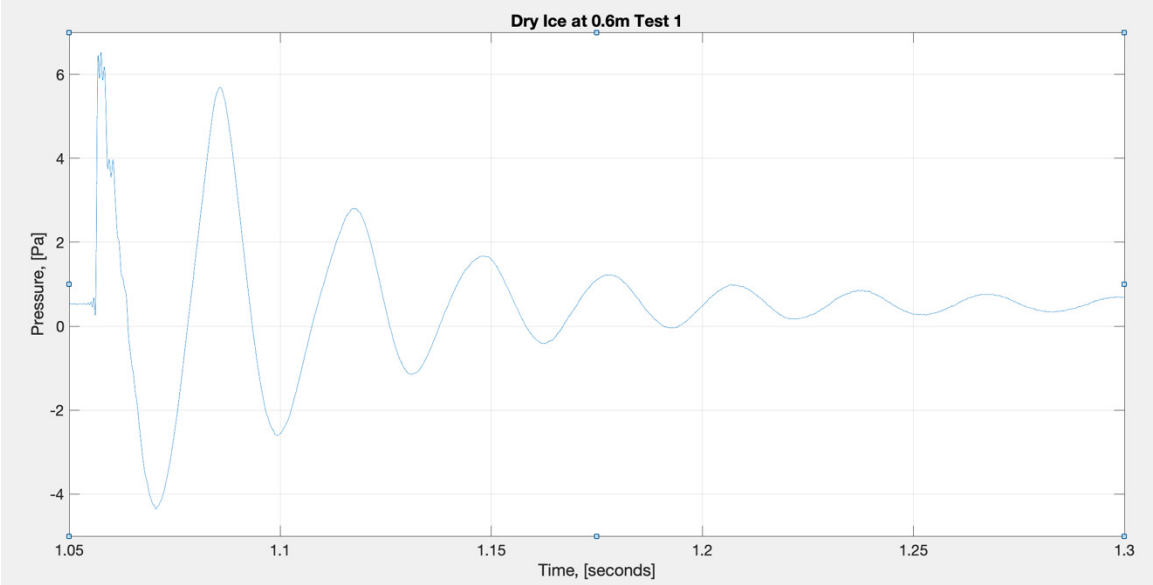

Figure 14. Dry ice at 0.6m test 1 zoomed.

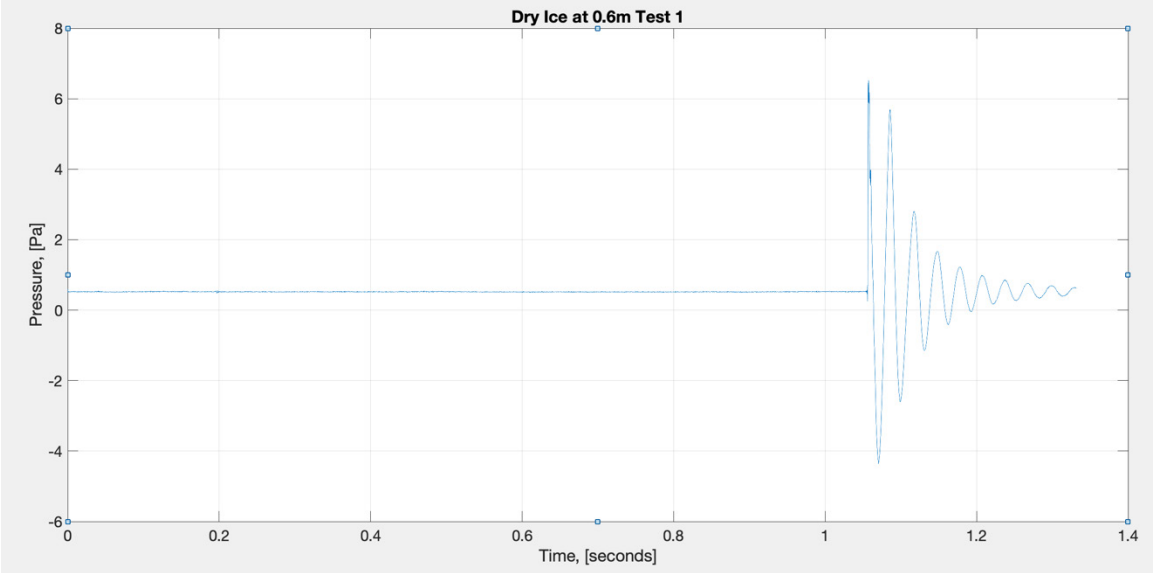

Figure 15. Dry ice at 0.6m test 1.

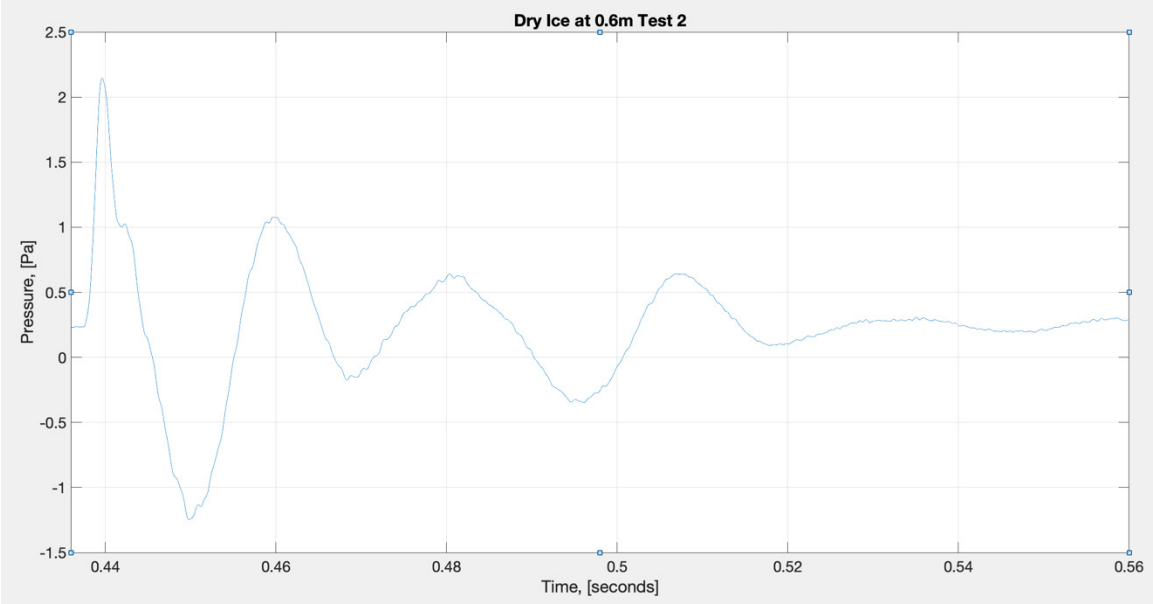

Figure 16. Dry ice at 0.6m test 2 zoomed.

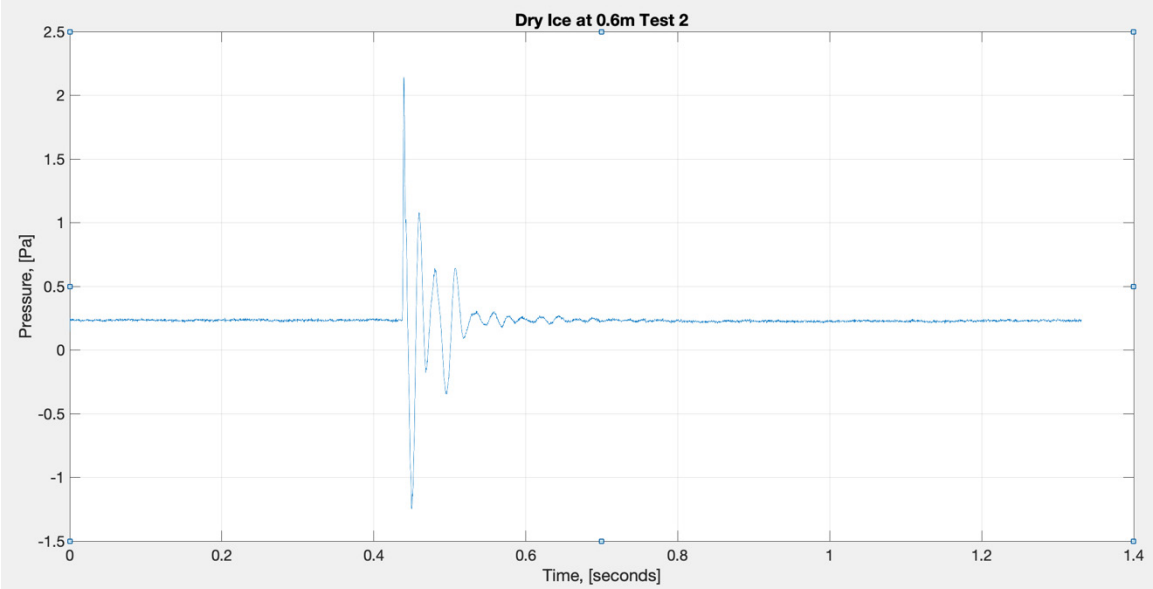

Figure 17. Dry ice at 0.6m test 2.

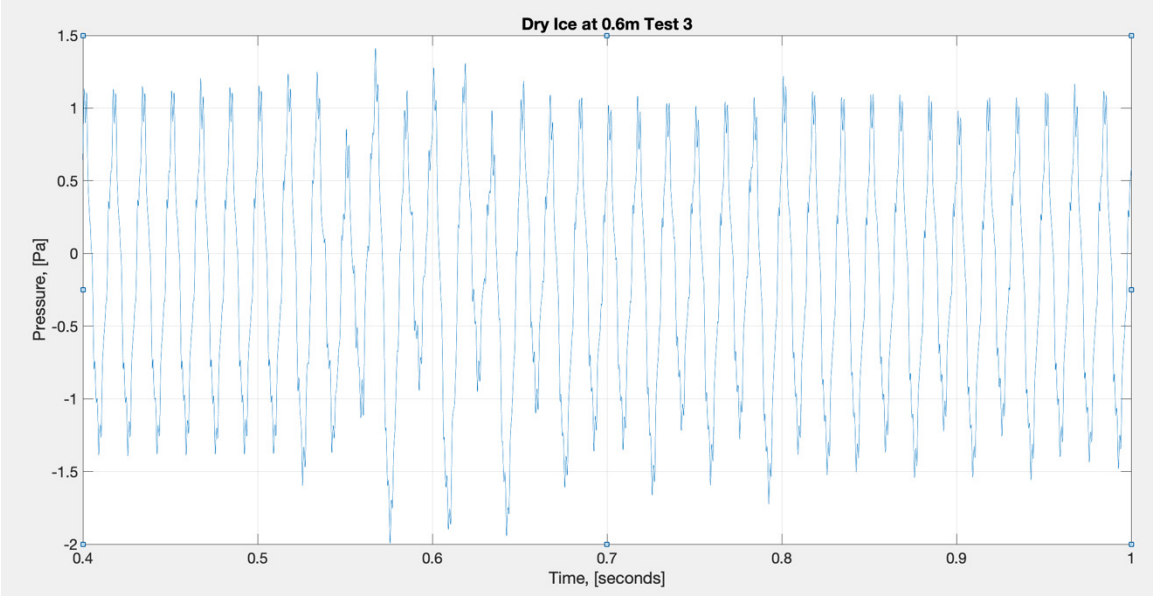

Figure 18. Dry ice at 0.6m test 3 zoomed.

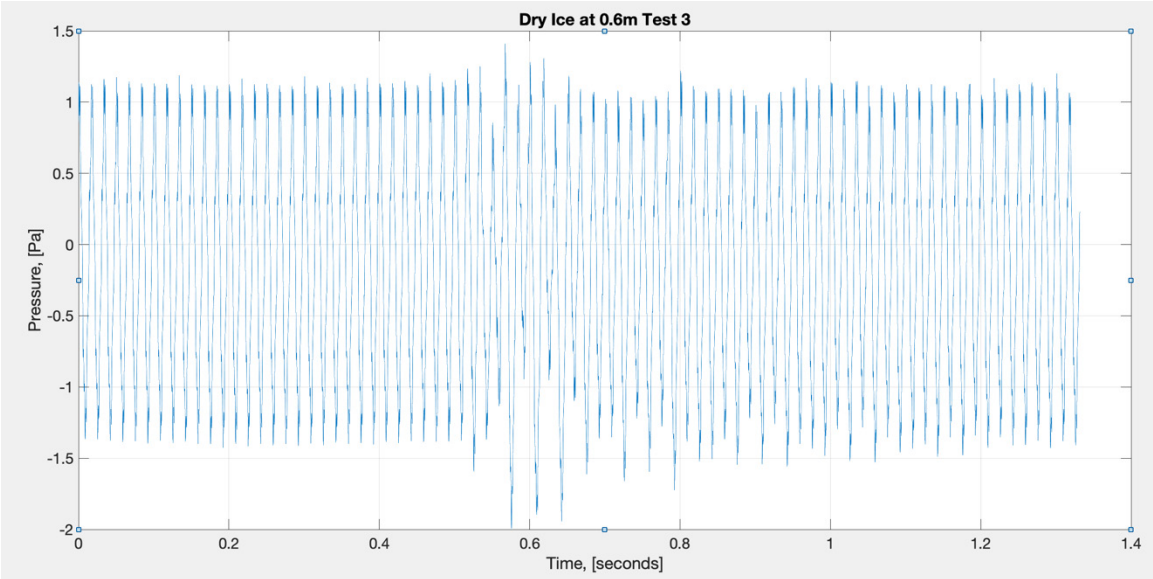

Figure 19. Dry ice at 0.6m test 3.

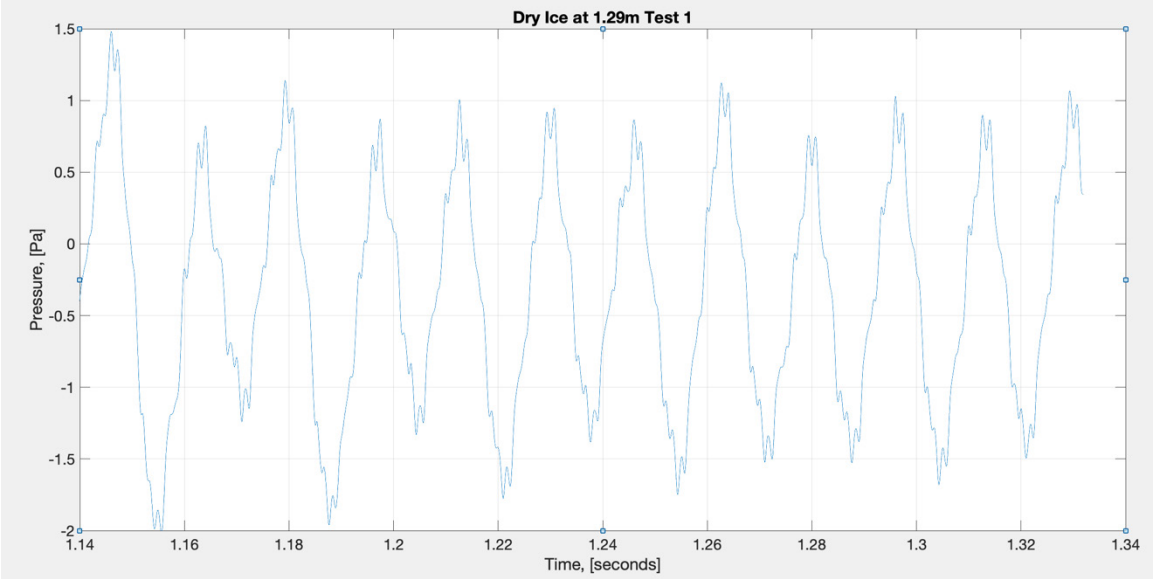

Figure 20. Dry ice at 1.29m test 1 zoomed.

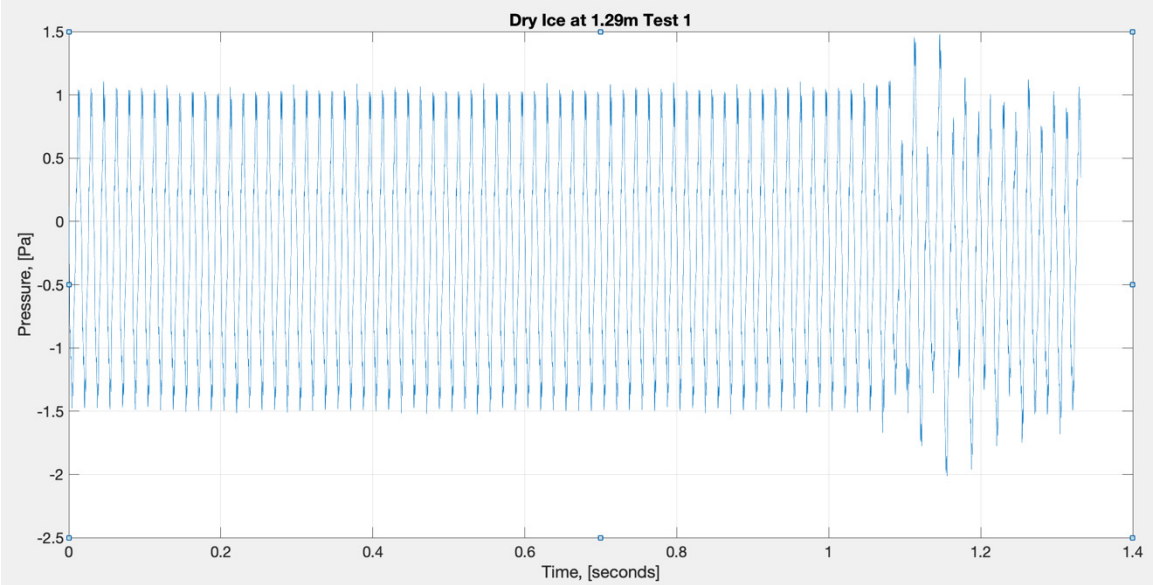

Figure 21. Dry ice at 1.29m test 1.

Another interesting discovery was made while conducting experiments using dry ice. At 1.29m distance from the sensor, the peak pressure actually occurred at the second peak rather than the first. The second peak being higher was counter intuitive because it is not the first wave to hit the sensor. This means that something had to cause a larger onset in pressure later on in time during the experiment. The second higher peak seemed to happen repeatedly and predictably at a distance of 1.29m. Possibilities for this phenomenon will be discussed later on in more detail but was at first believed to be constructive interference. This can be seen in Figures 22–23 and Figures 24–25 and Figures 26–27.

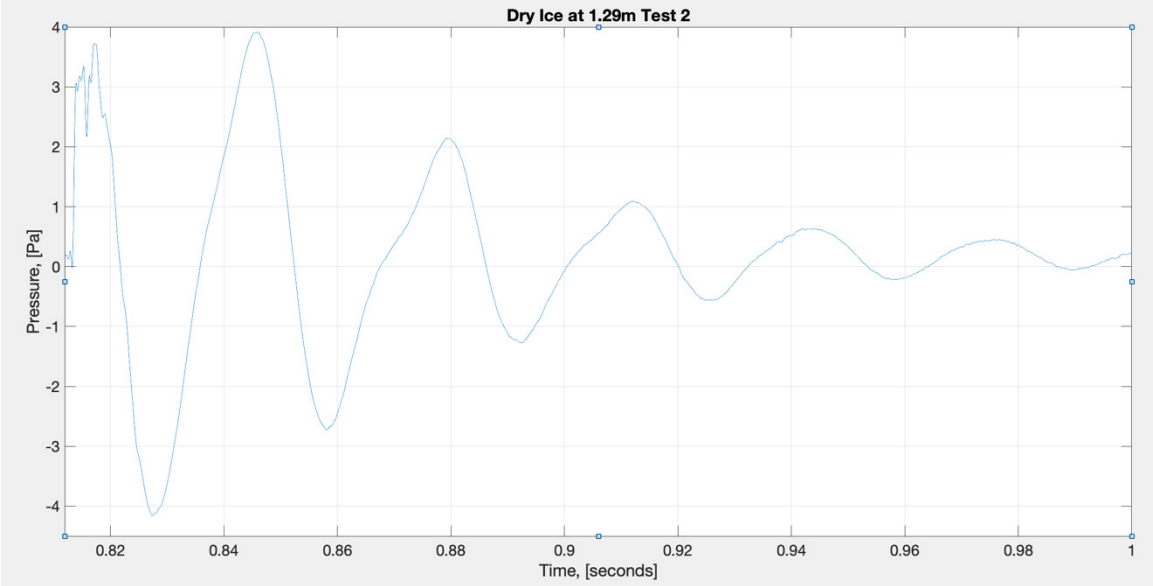

Figure 22. Dry ice at 1.29m test 2 zoomed.

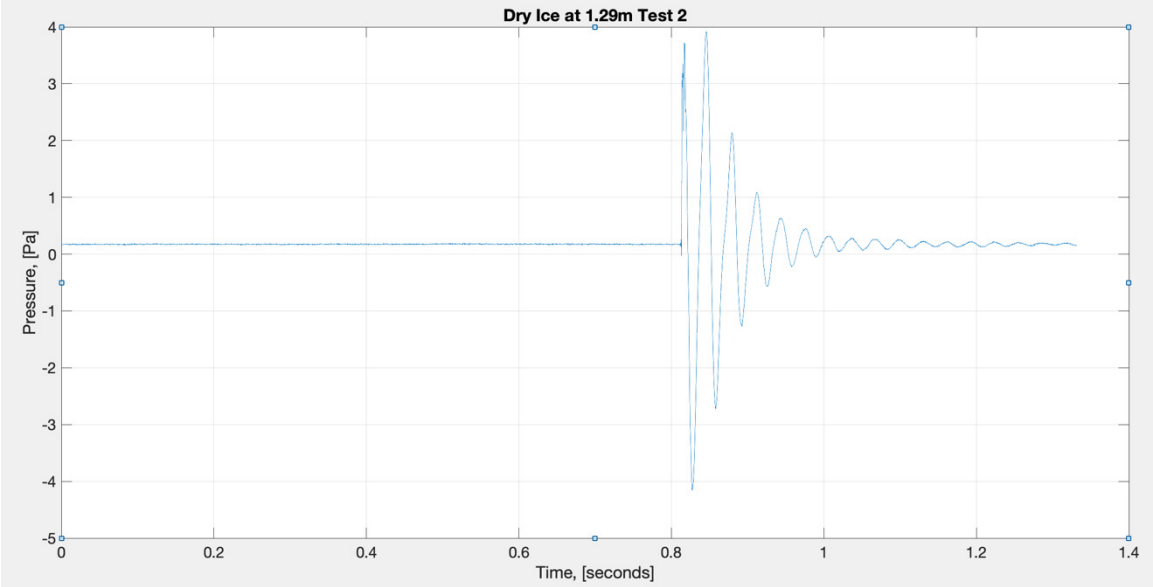

Figure 23. Dry ice at 1.29m test 2.

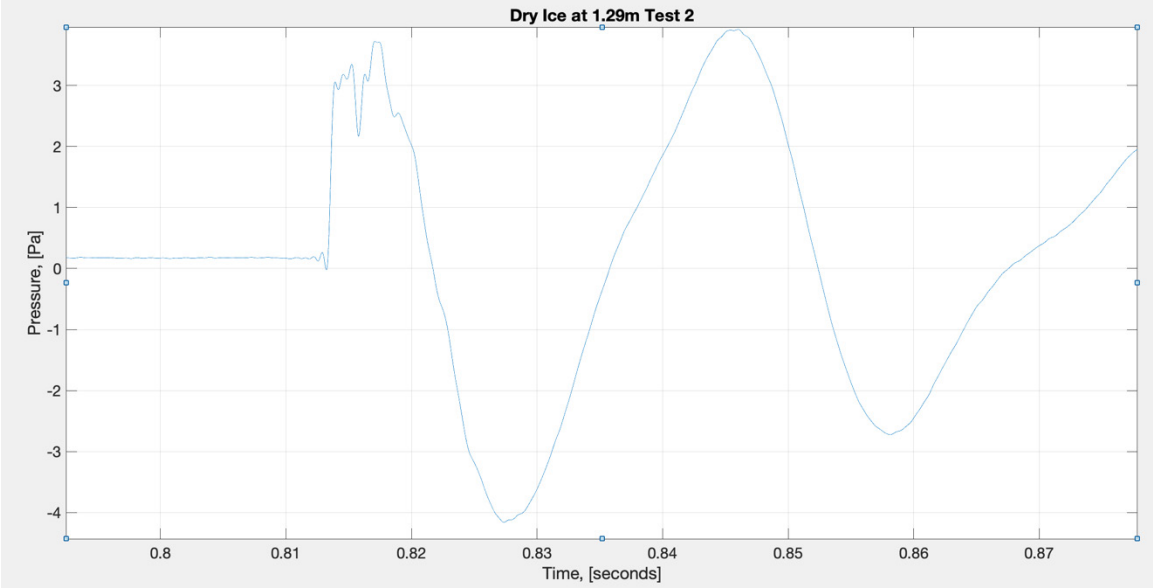

Figure 24. Dry ice at 1.29m test 2 second higher peak zoomed.

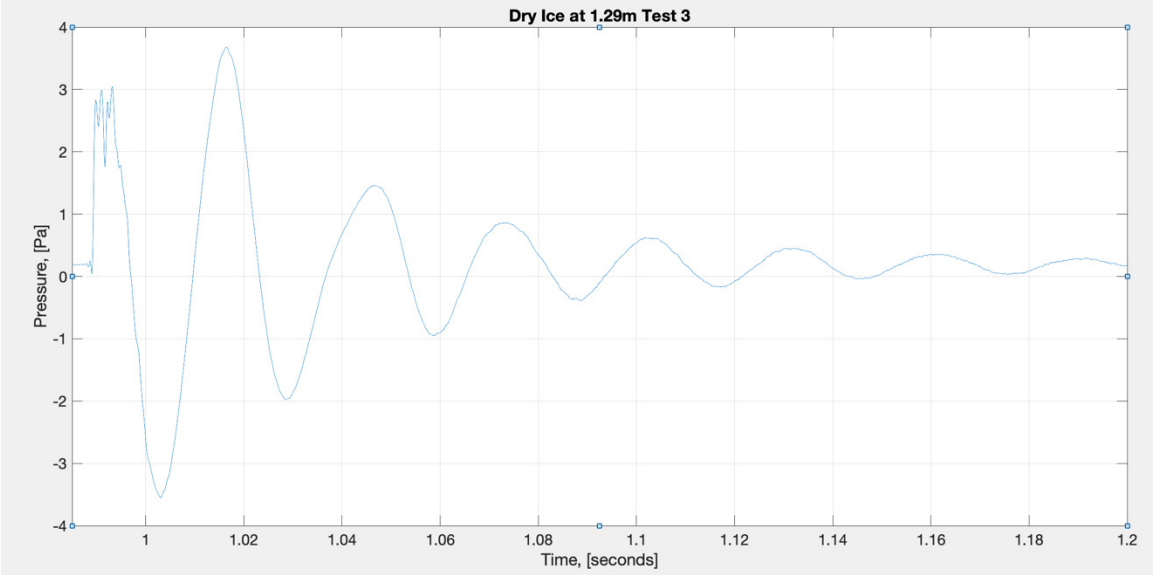

Figure 25. Dry ice at 1.29m test 3 zoomed.

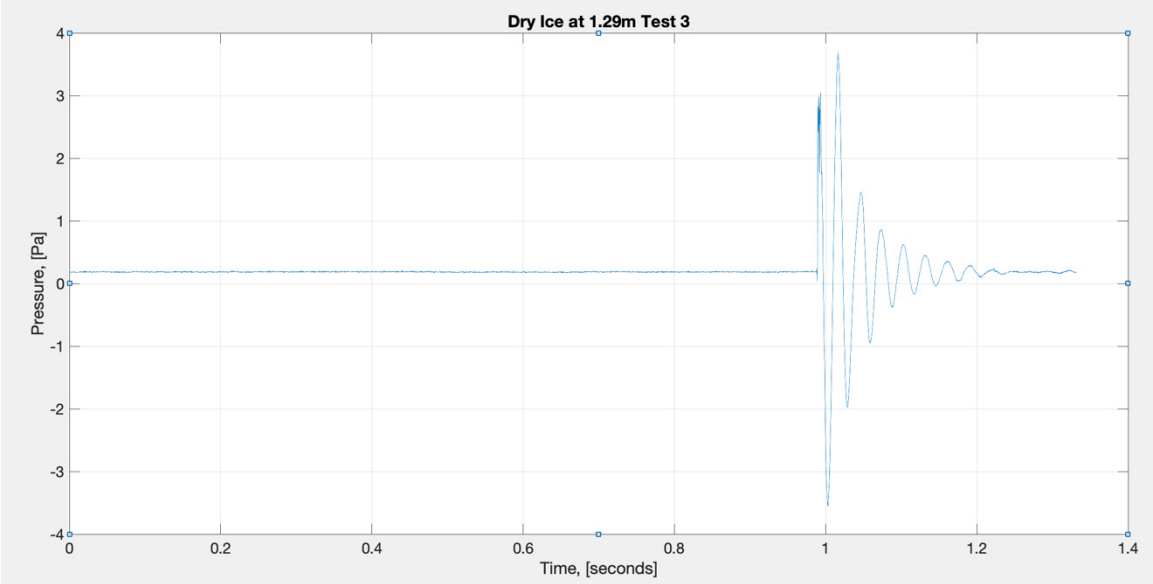

Figure 26. Dry ice at 1.29m test 3.

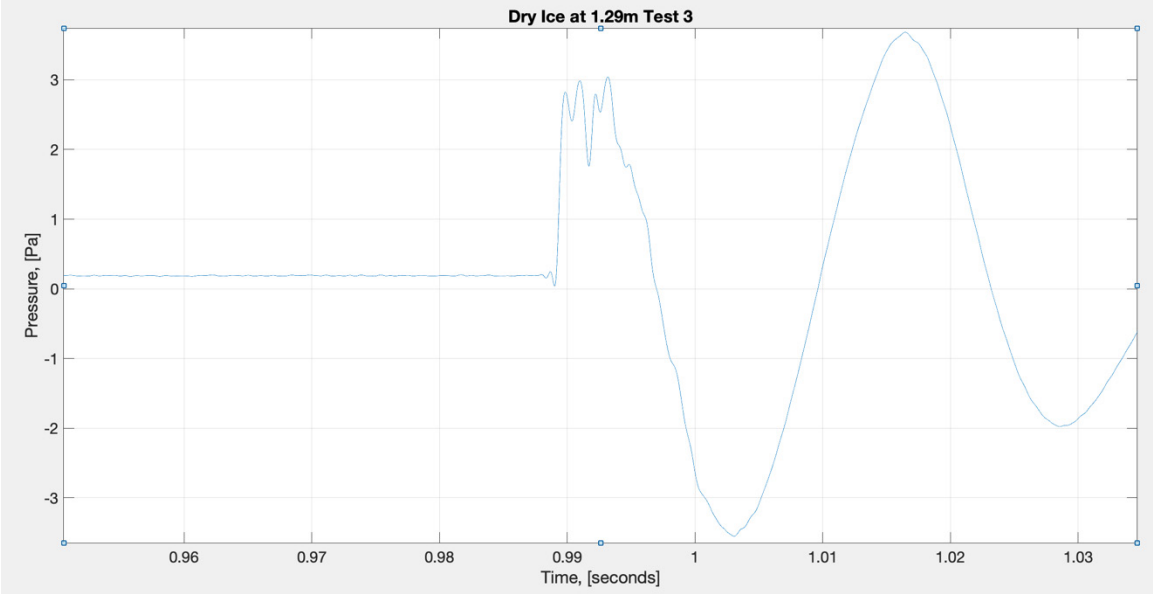

Figure 27. Dry ice at 1.29m test 3 second higher peak zoomed.

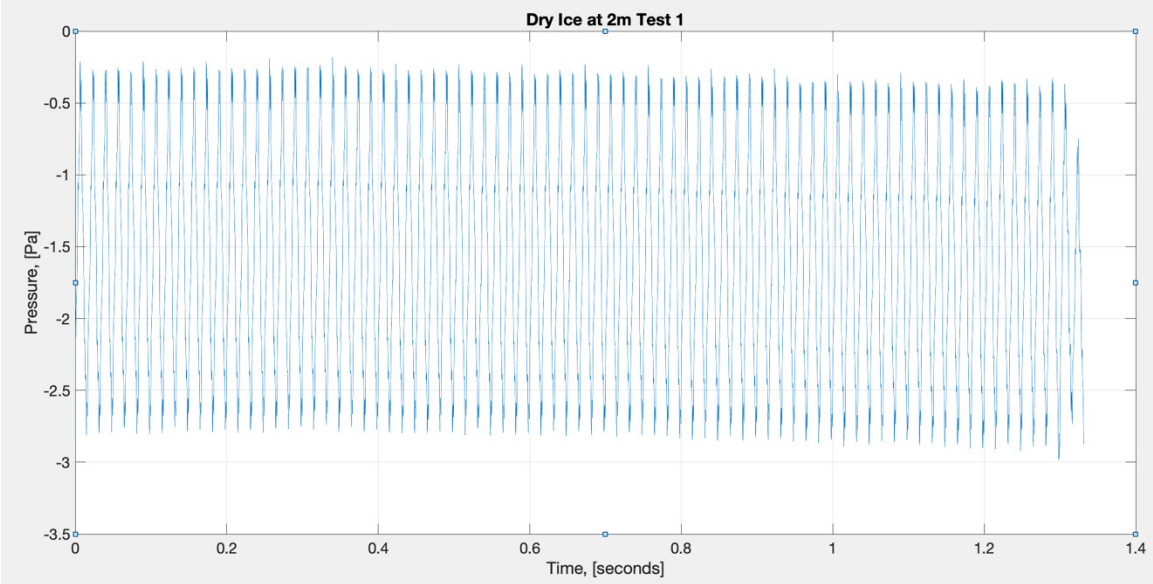

Figure 28. Dry ice at 2m test 1.

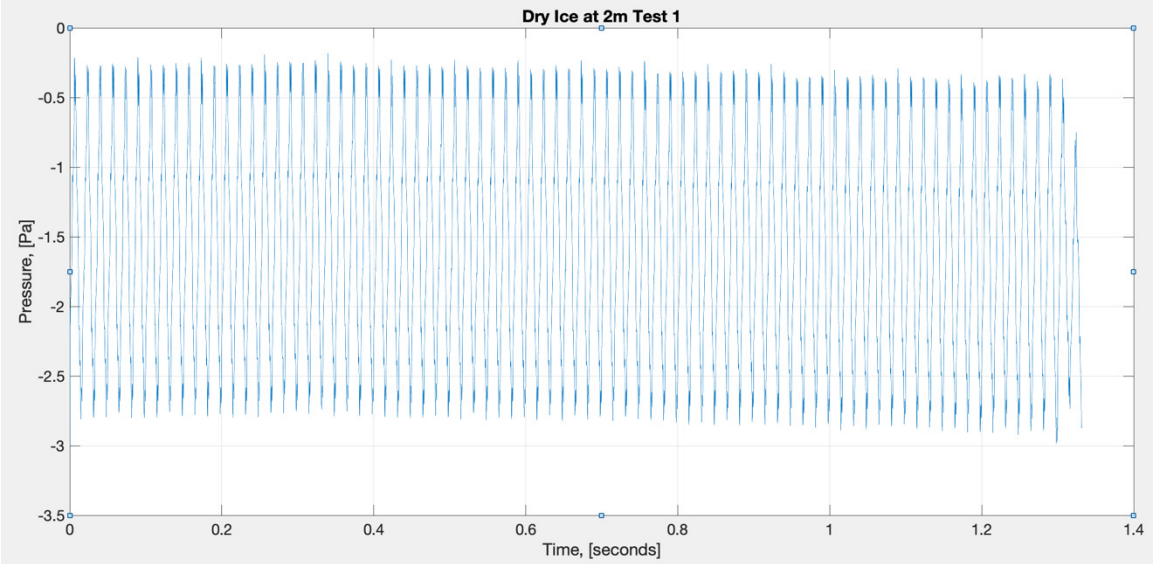

Figure 29. Dry ice at 2m test 1.

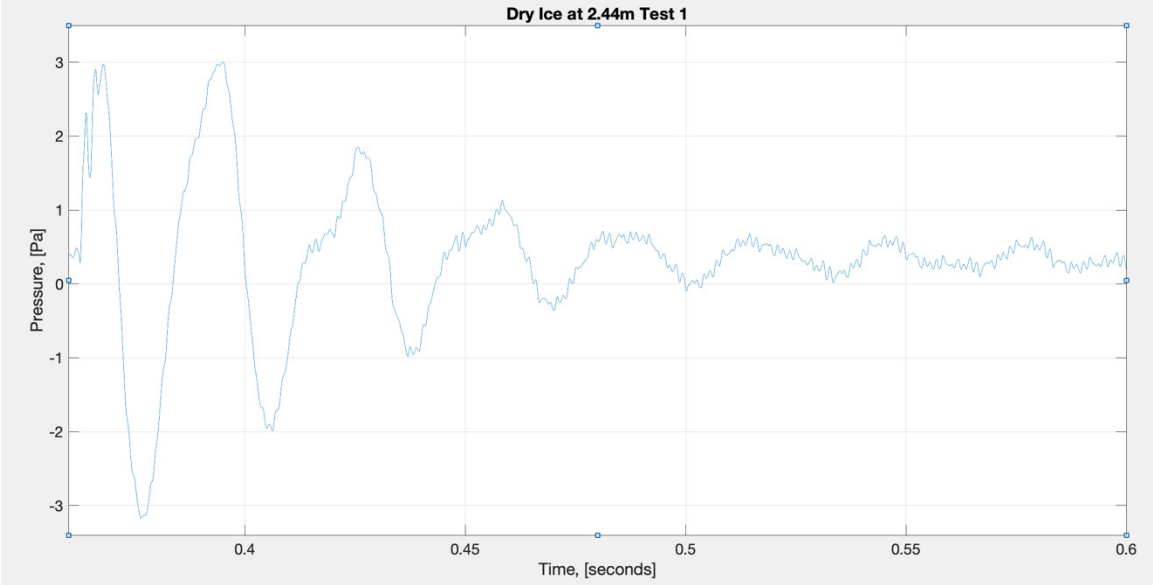

Figure 30. Dry ice at 2.44m test 1 zoomed.

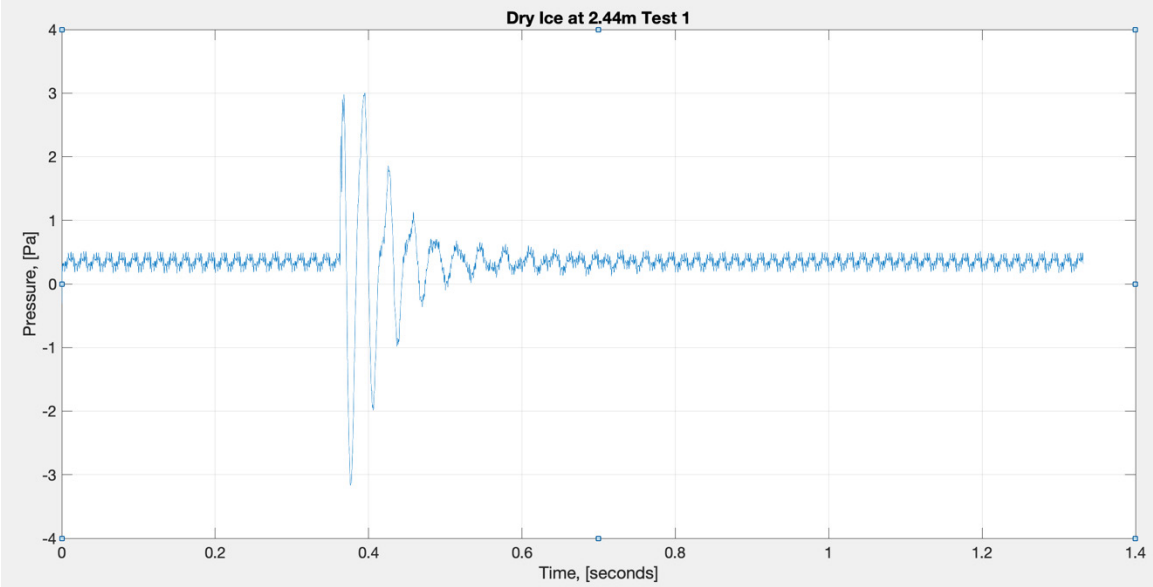

Figure 31. Dry ice at 2.44m test 1.

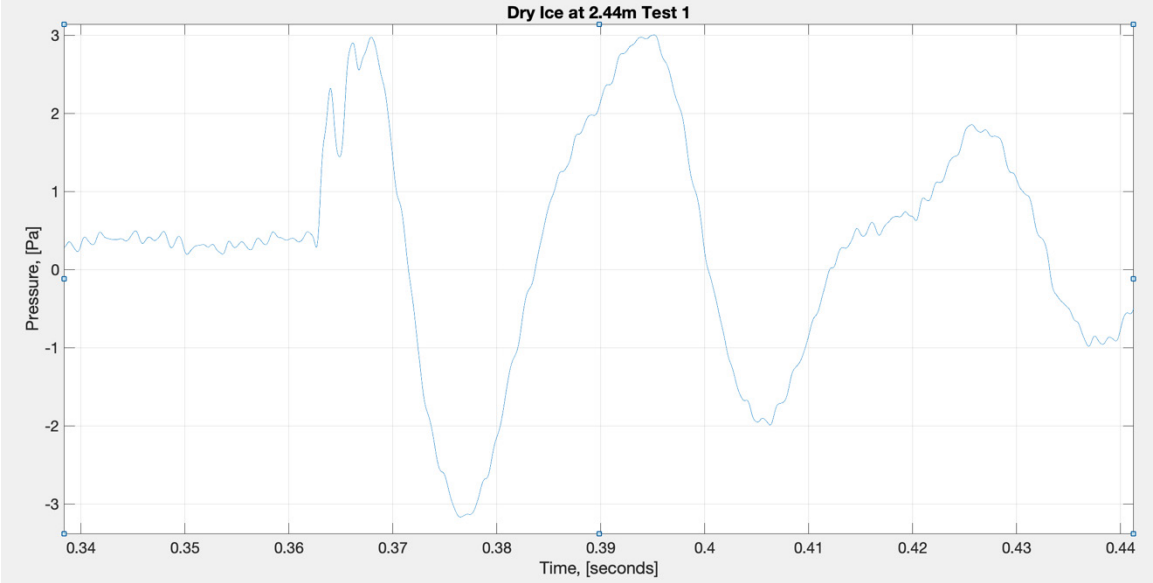

Figure 32. Dry ice at 2.44m test 1 second higher peak zoomed.

B. LIQUID NITROGEN

Liquid nitrogen testing exhibited results with less noise when compared to dry ice. This is likely due to the fact that no water was placed inside the pressure vessel, leaving only the expanding gasses to cause the rupture and resulting peak pressures. The expanding

gas was easier to keep constant. A constant amount of 100ml of liquid nitrogen was used for each test. Overall liquid nitrogen had a lower noise response and was able to be plotted very easily. A filtered response for a liquid nitrogen test at .6m can be seen in Figures 33 and 34.

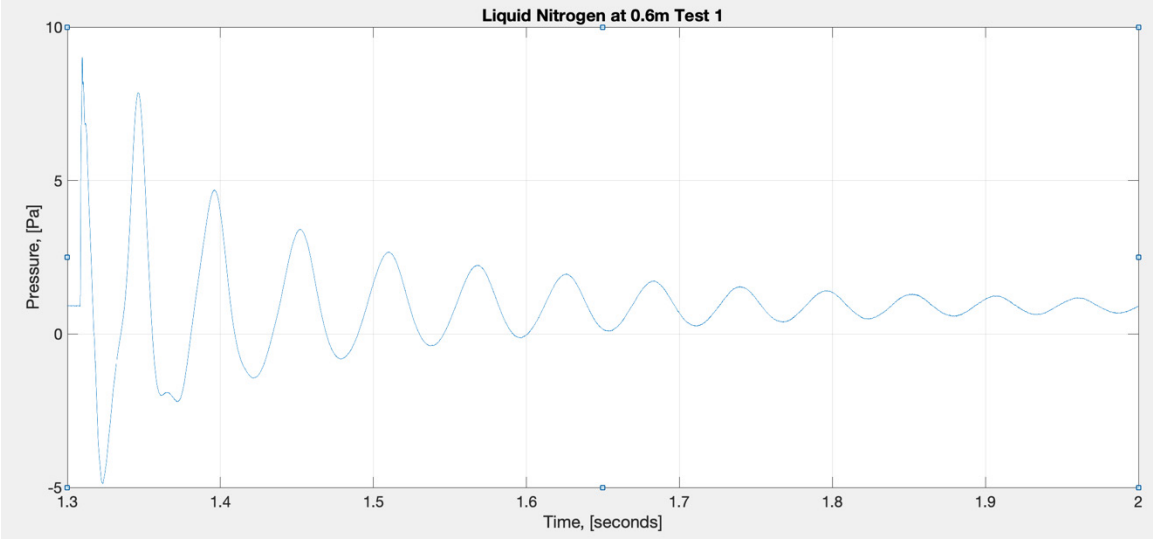

Figure 33. Liquid nitrogen at 0.6m test 1 zoomed.

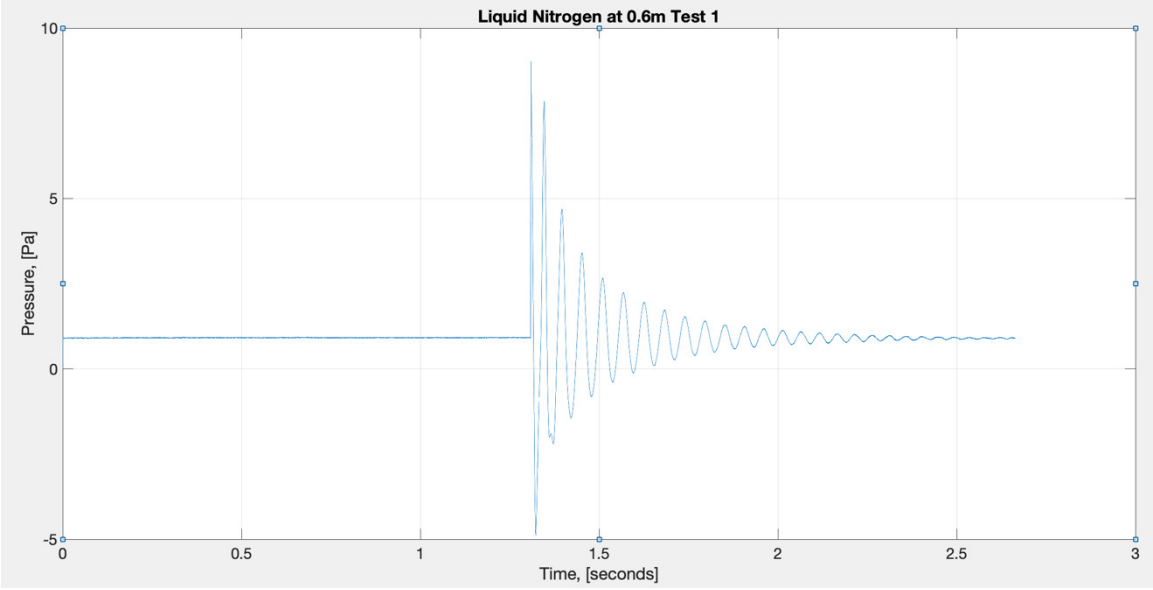

Figure 34. Liquid nitrogen at 0.6m test 1.

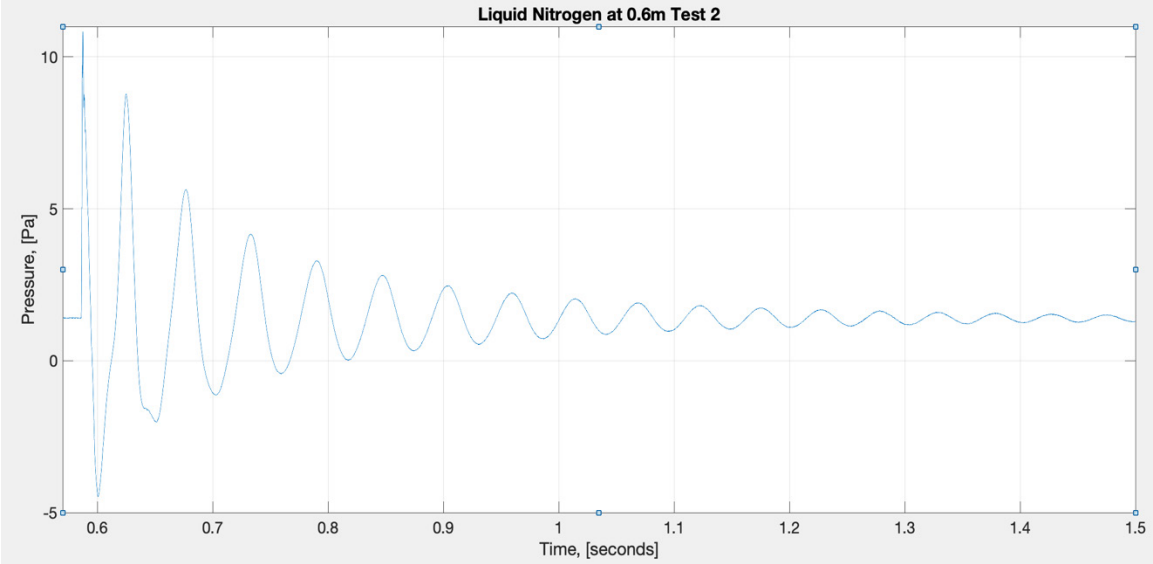

Figure 35. Liquid nitrogen at 0.6m test 2 zoomed.

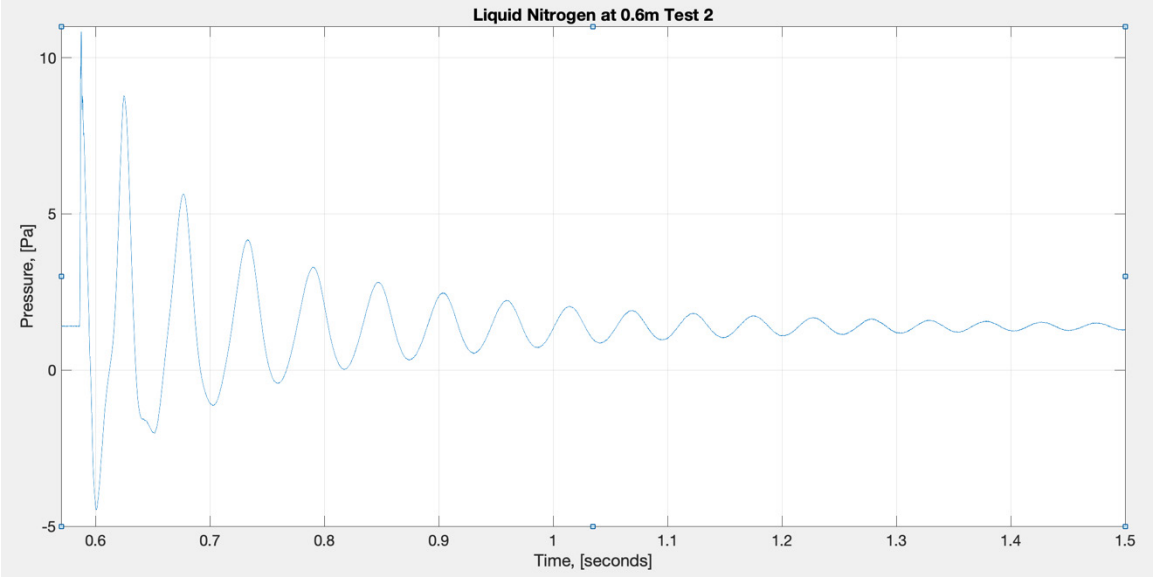

Figure 36. Liquid nitrogen at 0.6m test 2.

Liquid nitrogen ruptures happened faster than those using dry ice. This caused the occasional test to be slightly skewed as the pressure vessel was still sinking on its tethered weight down in the water column. This can clearly be seen in Figure 38.

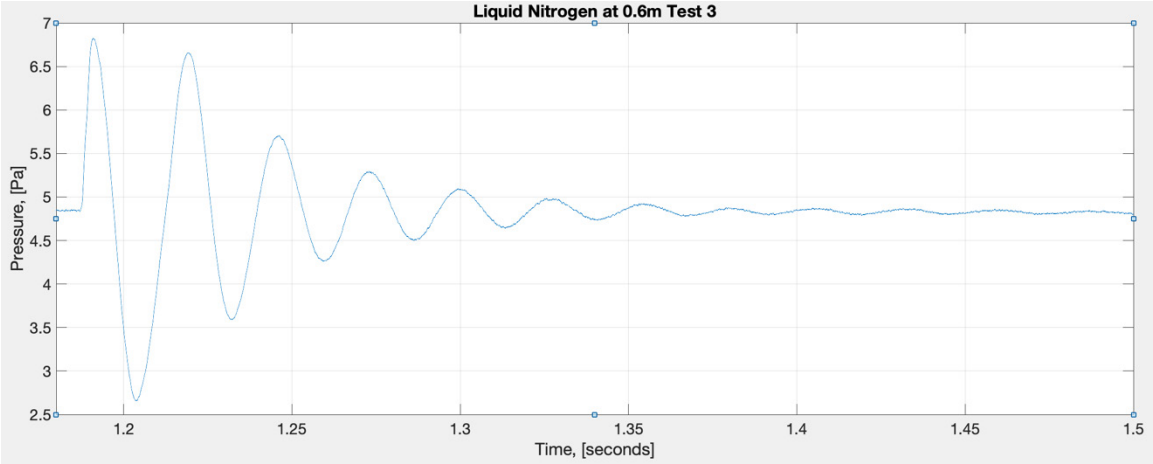

Figure 37. Liquid nitrogen at 0.6m test 3 zoomed.

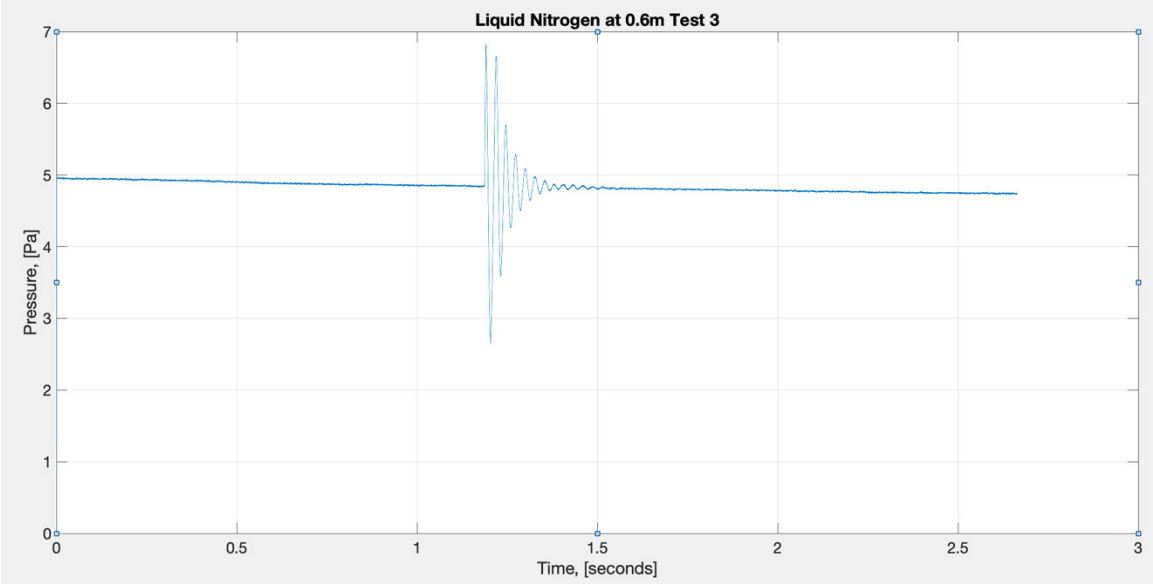

Figure 38. Liquid nitrogen at 0.6m test 3.

Similar to dry ice testing, liquid nitrogen testing can also be seen to have a higher second peak response at 1.29m. It is interesting to see how this phenomenon occurs repeatedly at 1.29m regardless of the medium used. This can be seen for liquid nitrogen testing in Figures 39–44.

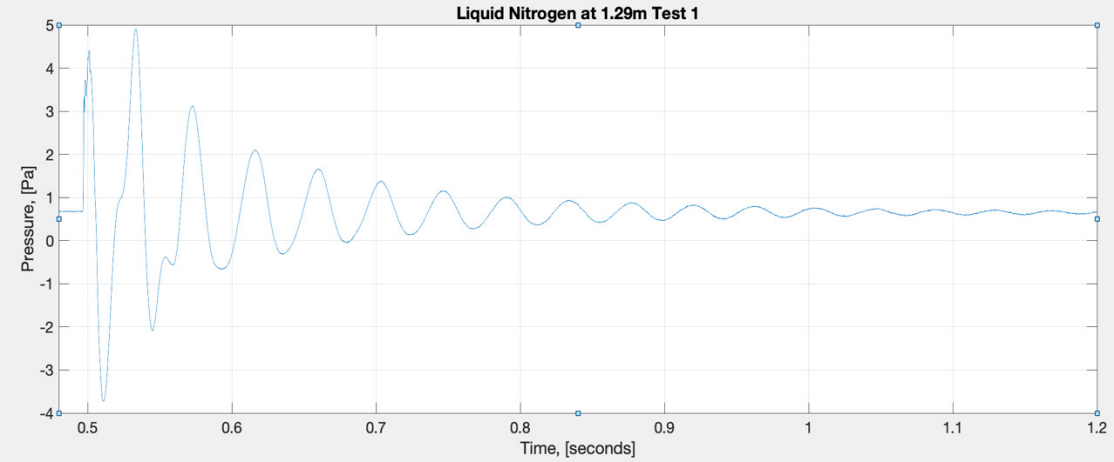

Figure 39. Liquid nitrogen at 1.29m test 1 zoomed.

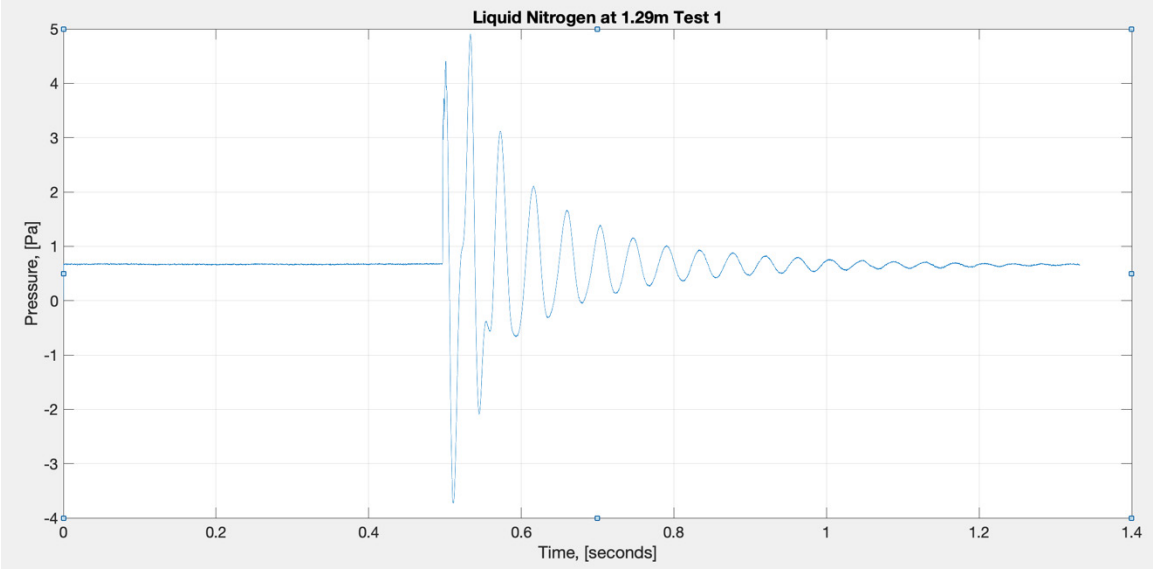

Figure 40. Liquid nitrogen at 1.29 test 1.

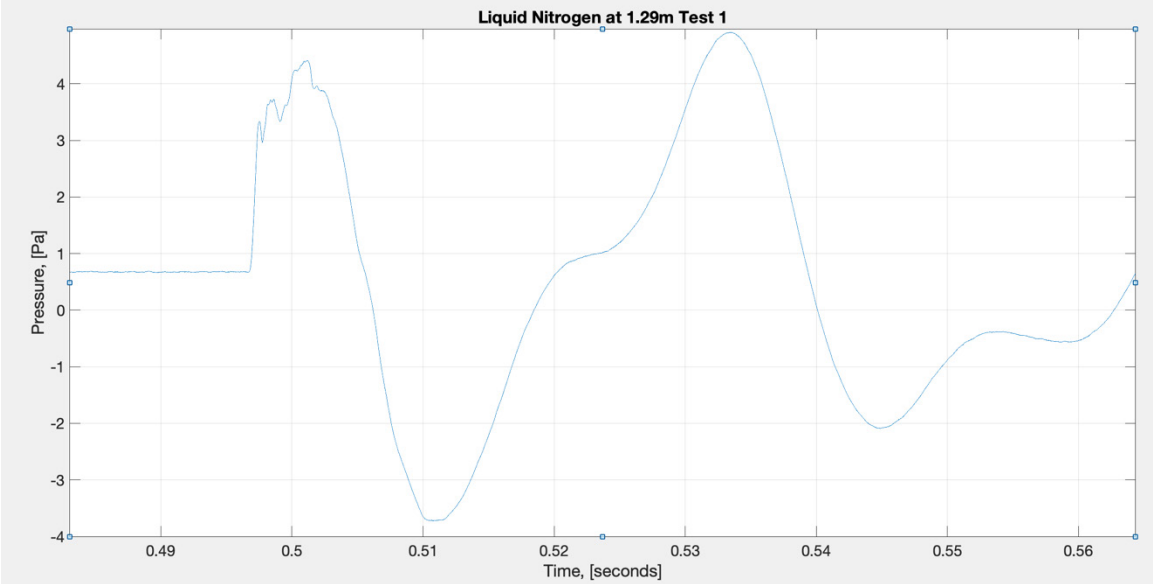

Figure 41. Liquid nitrogen at 1.29m test 1 second higher peak zoomed.

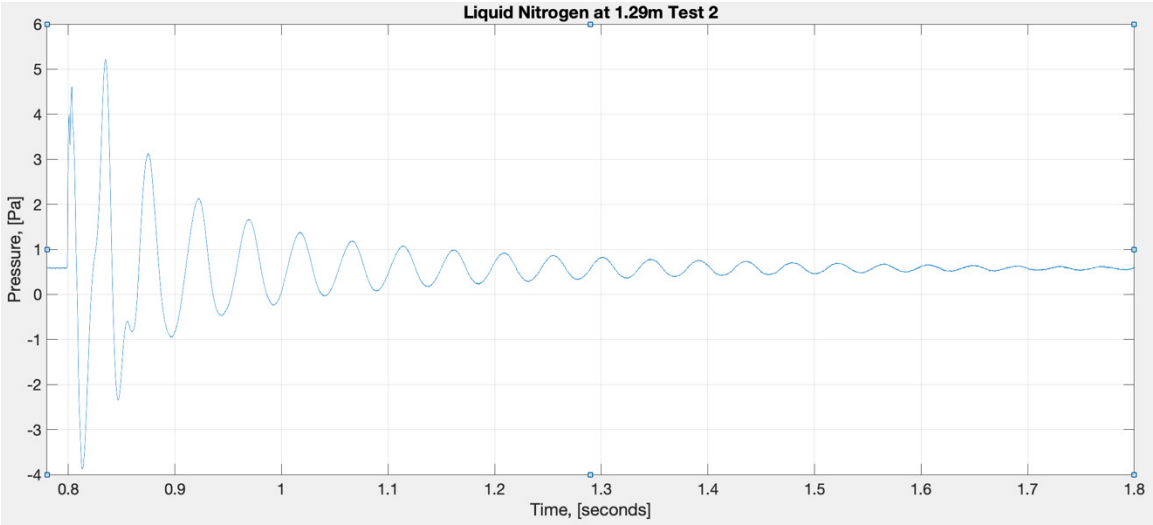

Figure 42. Liquid nitrogen at 1.29m test 2 zoomed.

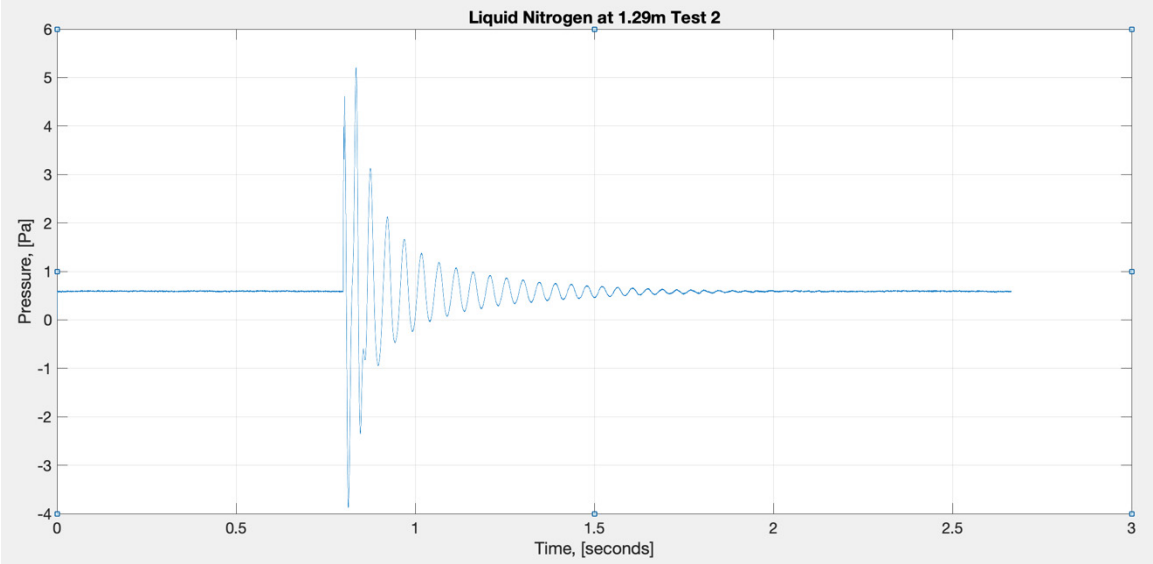

Figure 43. Liquid nitrogen at 1.29m test 2.

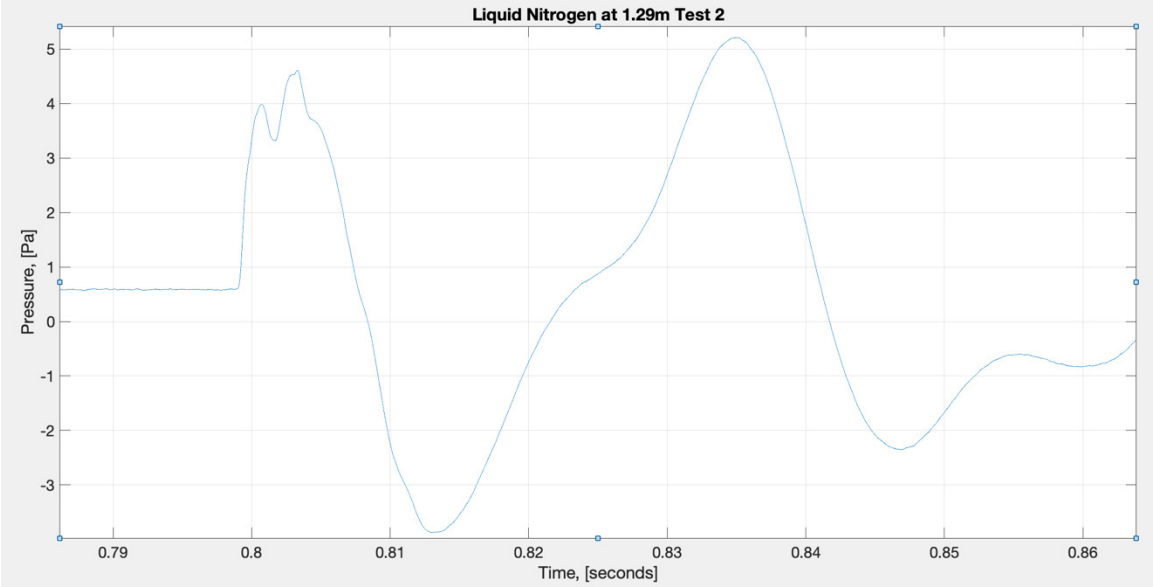

Figure 44. Liquid nitrogen at 1.29m test 2 second higher peak zoomed.

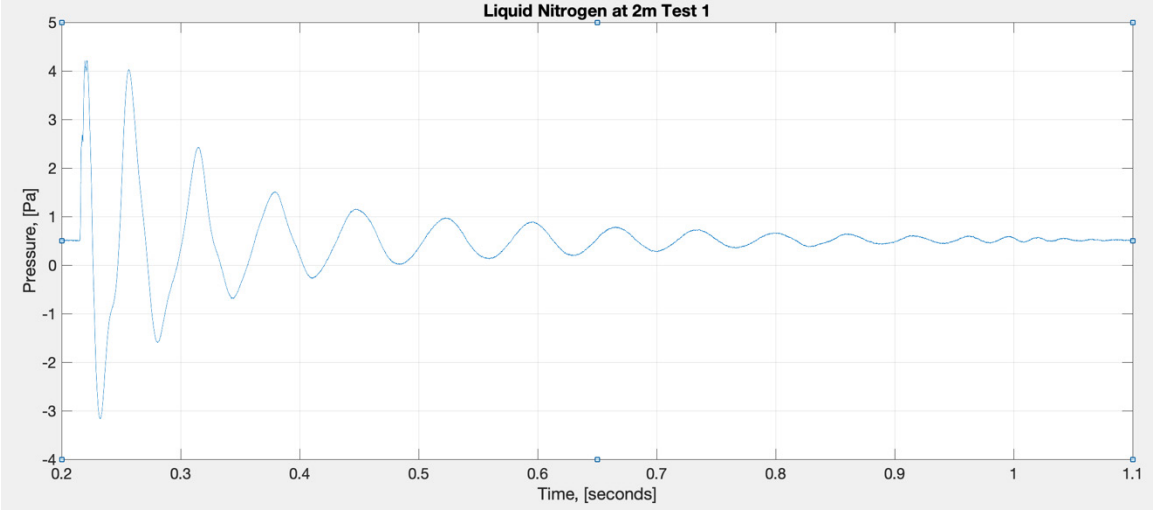

Figure 45. Liquid nitrogen at 2m Test 1 zoomed.

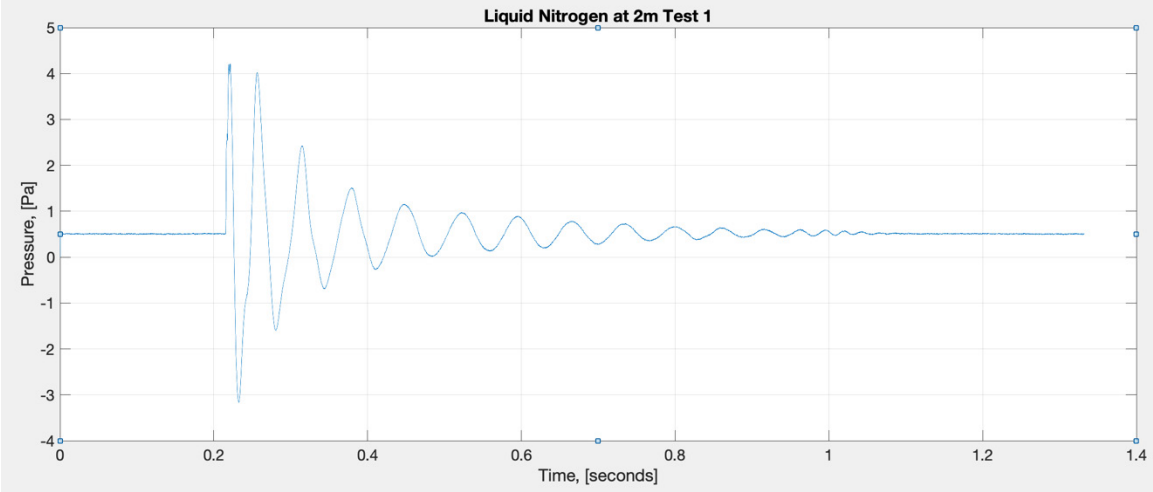

Figure 46. Liquid nitrogen at 2m test 1.

Certain liquid nitrogen tests had pulsations in pressure in the first peak similar to the ones found during dry ice testing. These pulsations were originally thought to be noise but upon further analysis and filtering were persistent and clearly visible as seen in Figures 40–48.

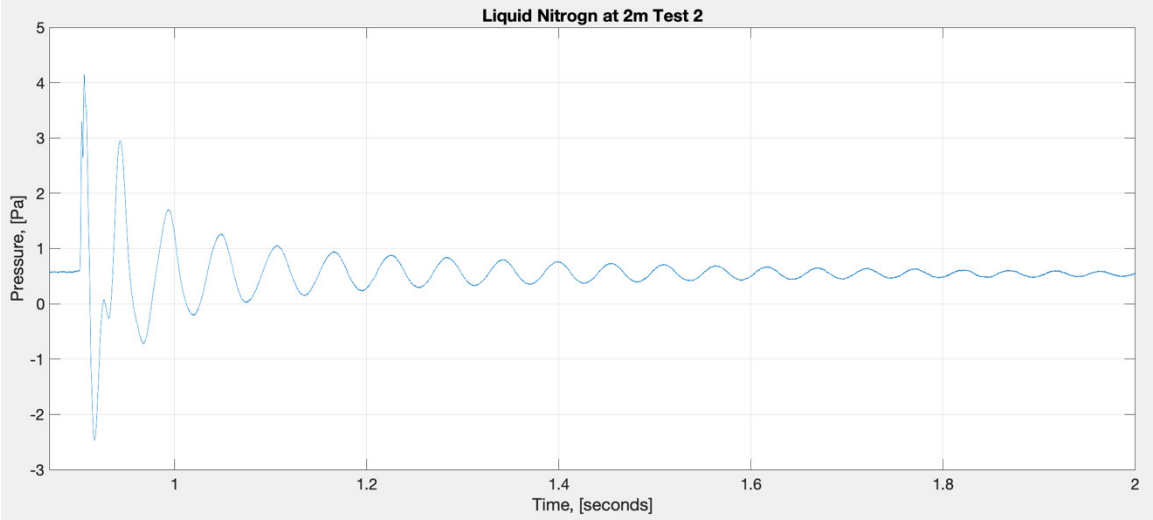

Figure 47. Liquid nitrogen at 2m test 2 zoomed.

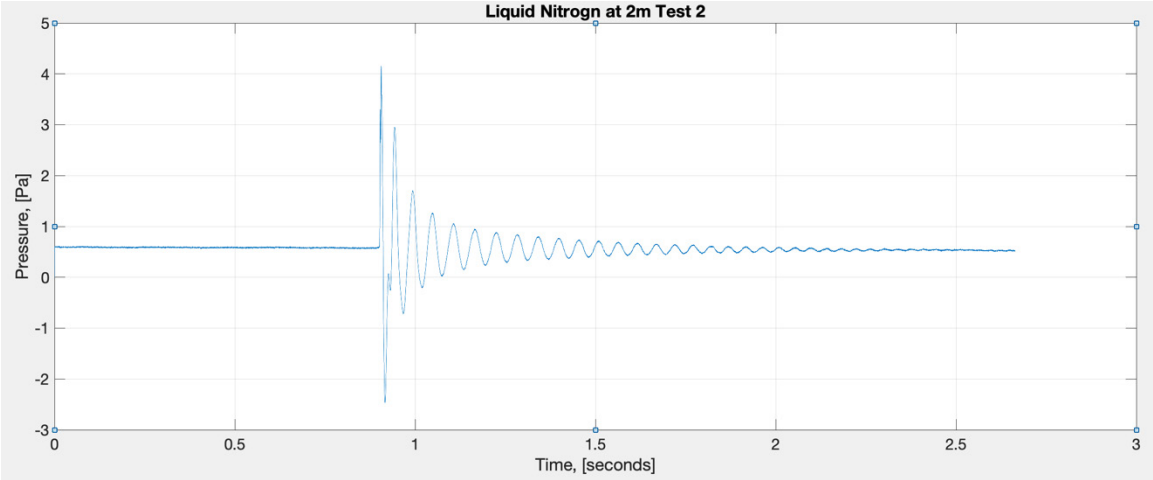

Figure 48. Liquid nitrogen at 2m test 2.

C. DRY ICE AND LIQUID NITROGEN SLOPE

Average slopes for all tests and distances for both dry ice and liquid nitrogen can be seen in Table 1. In general, liquid nitrogen took slightly longer to reach peak pressure than dry ice. The one exception to this had to do with the second higher peak at 1.29m. At that distance, the liquid nitrogen was faster than dry ice in reaching the second higher peak. It is possible this is due to how the bubble was formed by the different mediums, with one test including gas only, and the other including gas and water. This Table 1 also helps to

validate the Po curve plotted above as seen in Figures 6 and 8. As the pressure vessel moves further away from the sensor the rate or slope is smaller, meaning it takes more time to travel through the water. Less pressure and more time equate accurately to what is expected at further distances.

Table 1. Dry ice and liquid nitrogen slope.

Dry Ice Slope	Pa/Sec	Liquid Nitrogen Slope	Pa/Sec
0m	4726.75	0m	4612.62
.6m	3877.65	.6m	3782.23
1.29m	2531.23	1.29m	2334.71
2m	2213.22	2m	2037.63
Dry Ice Second Higher Peak Slope	Pa/Sec	Liquid Nitrogen Second Higher Peak Slope	Pa/Sec
Test 2 1.29m	434.93	Test 1 1.29m	479.43
Test 3 1.29m	436.88	Test 2 1.29m	474.61

THIS PAGE INTENTIONALLY LEFT BLANK

IV. IMPLOSION TESTING

Implosion testing was challenging to perform and isolate from an actual explosion. The study of the collapsing underwater "bubble" created by an explosion and the damaging effects that come with it to ships has been of great interest to the USN and DoD for years. I decided to test this using a standard USN weather balloon, as seen in Figure 49. I theorized that filling the balloon with air, placing it in a water column, and rapidly rupturing it would test for implosion without needing an explosion first. If this could be done, it would prevent the need to filter out explosion data in order to analyze only the implosion. This would allow for more accurate testing of the damaging effects of the implosion and the underwater bubble alone.

The center of the balloon was placed 1.29m above the floor of the tank and 1.29m below the surface of the tank. Each of the four walls were 1.29m from the center of the balloon. The balloon was weighed down with 22.5Kg of lead weight to overcome the force of buoyancy. The balloon was then punctured rapidly with a sharp object and allowed to collapse fully under the water column pressure alone. The sensor was in contact with the edge of the balloon when the rupture occurred. The sensor did not pick up a change in pressure and therefore the test and data obtained from it was deemed to be inconclusive. Ideas for how to proceed with this type of testing will be covered in a later chapter.

Figure 49. USN weather balloon (1m in diameter)

V. RESULTS AND DISCUSSION

A. SECOND HIGHER PEAK 1.29M

During testing, I had several possible theories on why the peak pressure occurred during the second peak at 1.29m. I thought that the pressure vessel was rupturing inconsistently and the pressure sensor was receiving a pre-mature shock front. It is possible that the cap of the pressure vessel was rupturing or coming off first and could have made the first peak lower in pressure. This however did not explain the second higher peak occurring at the same distance every time. A typical ruptured pressure vessel can be seen in Figures 53 and 54. The pressure vessels seemed to rupture with a zippering-like effect consistently during all testing. This made the cap rupturing or a pre-mature shock wave theory of any kind unlikely. The cap can be seen fully intact in Figures 53 and 54.

The next theory that could have caused this second higher shock peak was constructive interference. This could have been caused by the bottom of the tank reflecting a pressure wave. If the reflection was happening at the right angle then it could have come back into contact with the already propagating pressure waves causing the waves to compound on top of each other and create a higher pressure. Though the tank used to conduct this testing is designed to mitigate propagation, it still can happen. This can be seen in Figure 52.

Conducting testing at 1.29m was initially thought to be a bad distance to test at and was initially avoided after this second higher peak continued to occur. Eventually it was noted that it might be a great distance to test at specifically for ships operating in shallow water environments or littorals. The Littoral Combat Ship, (LCS) class of USN ships operates in shallow water environments to conduct anti-submarine and mine warfare [7]. The way the two classes of ships differ in hull structure makes it important to analyze both ships' responses to underwater explosion events. Picking the best ship for the best mission will places sailors in a safer environment with a ship that has a larger chance of survival [8], [9]. This specific distance is also relevant to testing critical infrastructure placed in shallow water such as tunnels and communication cabling.

B. PULSATIONS IN PRESSURE AT THE FIRST PEAK

Pulsations were first seen after dry ice data was successfully filtered using MATLAB. With liquid nitrogen testing these pulsations could be seen without filtering the data. The consistency in these pulsations between the two mediums provided reassurance that they were not noise, but rather a possible bubble pulse as it traversed through the water column [10]. This can be seen for a typical USN shock trial size explosion happening in Figure 50,51 [11].

The sensor was sometimes known to shift during testing. Since there was only one sensor used for testing it was assumed that the pulsations could be from the sensor shifting slightly and picking up a new shock wave while still trying to record the previous one. This will be easily tested and confirmed with the addition of multiple sensors.

C. DEVELOPING EQUATIONS AND CONSTANTS

Trinitrotoluene (TNT) has been widely used for underwater explosions. The USN switched to using a TNT like explosive called HBX-1 [12]. This switch was because HBX-1 had explosive qualities more in line with what the USN wanted to obtain in underwater explosions. These qualities can be seen in Table 3.

Equations to help better understand how underwater explosions occur have been extensively discussed by Cole as well as others [13],[14]. The DoD references them in several instructions and publications [15],[16]. These equations help to better calculate the effects of underwater explosions caused by certain explosives detonated underwater. These equations can be seen below where (W) is equal to charge weight in pounds (or pounds of TNT, HBX-1 etc., and R is equal to wave propagation in feet for a spherical charge. Pmax is for maximum peak pressure in PSI and the decay constant known as theta in mili seconds. K1, A1, K2, and A2 are constants specific to each type of explosive.

$$P_{max} = K_1 \left(\frac{W^{\frac{1}{3}}}{R} \right)^{A_1}$$

$$\theta = K_2 W^{\frac{1}{3}} \left(\frac{W^{\frac{1}{3}}}{R} \right)^{A_2}$$

The goal was to find the constants for dry ice and liquid nitrogen that would work in the equations above as well as be able to be added to Table 3. These equations are not linear and are not easily comparable. Dry ice and liquid nitrogen do not provide shock waves in the same manner as underwater explosives [14], [15]. This makes it challenging to apply the above equations.

Dry ice had an average Detonation Velocity of 410m/s while liquid nitrogen had an average Detonation Velocity of 206m/s.

Table 2. Dry ice and liquid nitrogen time to reach peak pressure.

Dry Ice Time to Reach Peak Pressure	Seconds	Liquid Nitrogen Time to Reach Peask Pressure	Seconds
0m	0.001	0m	0.004
.6m	0.002	.6m	0.005
1.29m	0.003	1.29m	0.006
2m	0.004	2m	0.007
Dry Ice Time to Reach Second Higher Peak	Seconds	Liquid Nitrogen Time to Reach Second Higher Peak	Seconds
Test 2 1.29m	0.033	Test 1 1.29m	0.033
Test 3 1.29m	0.027	Test 2 1.29m	0.027

D. NEGATIVE PRESSURE

All plots of dry ice and liquid nitrogen contained negative pressures as time elapsed toward a decay type response and eventually returning to 0 Pa in the filtered data or to the noise detection threshold in the un-filtered data. This was due to the sensor reading pressure changes in a differential mode set-up [16]. It was decided to take one graph of liquid

nitrogen and dry ice and plot it with only peak positive pressures to see how accurately the test appeared when compared to an actual underwater explosion event.

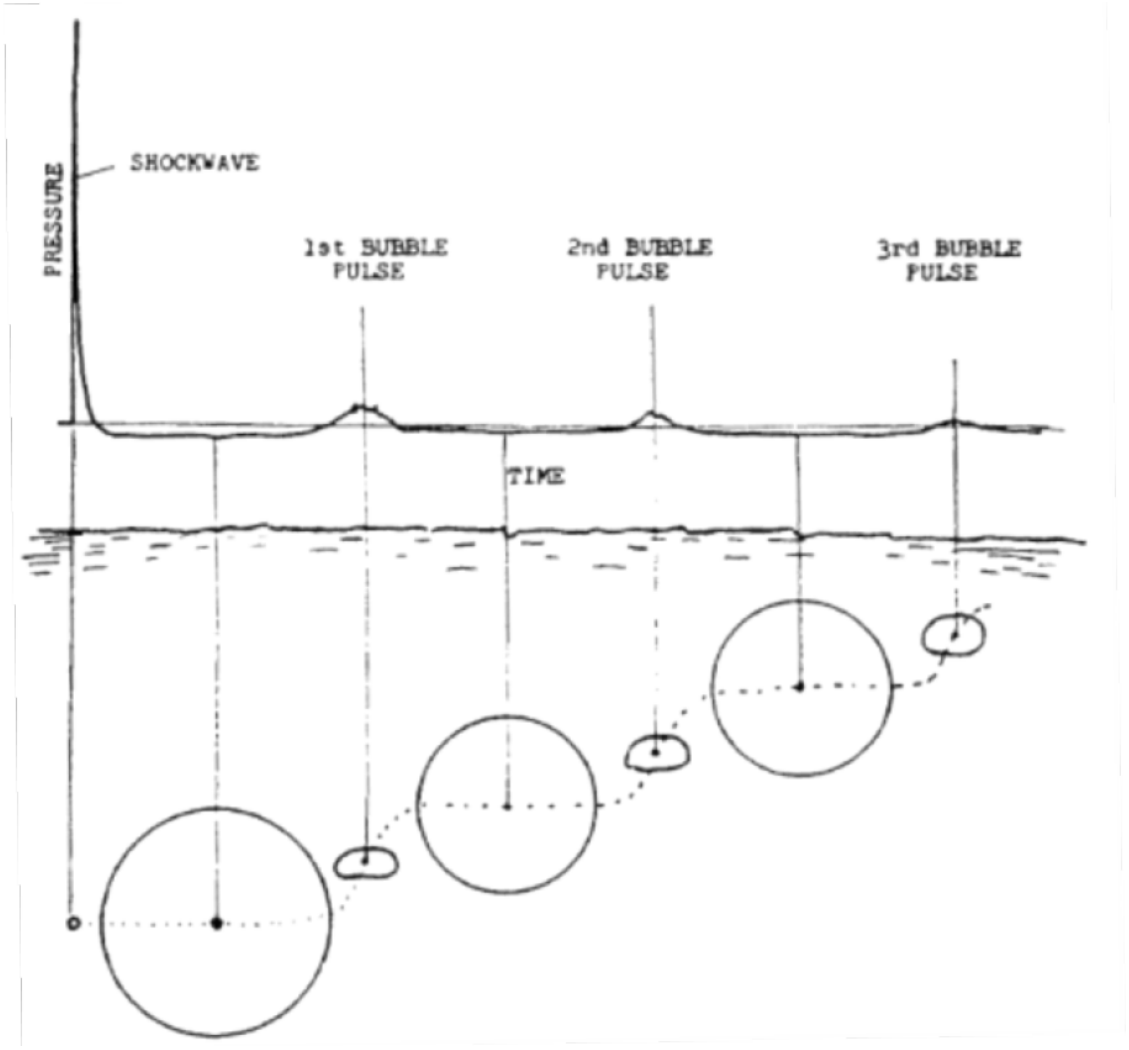

Figure 50. Bubble phenomena from underwater explosions. Source: [4].

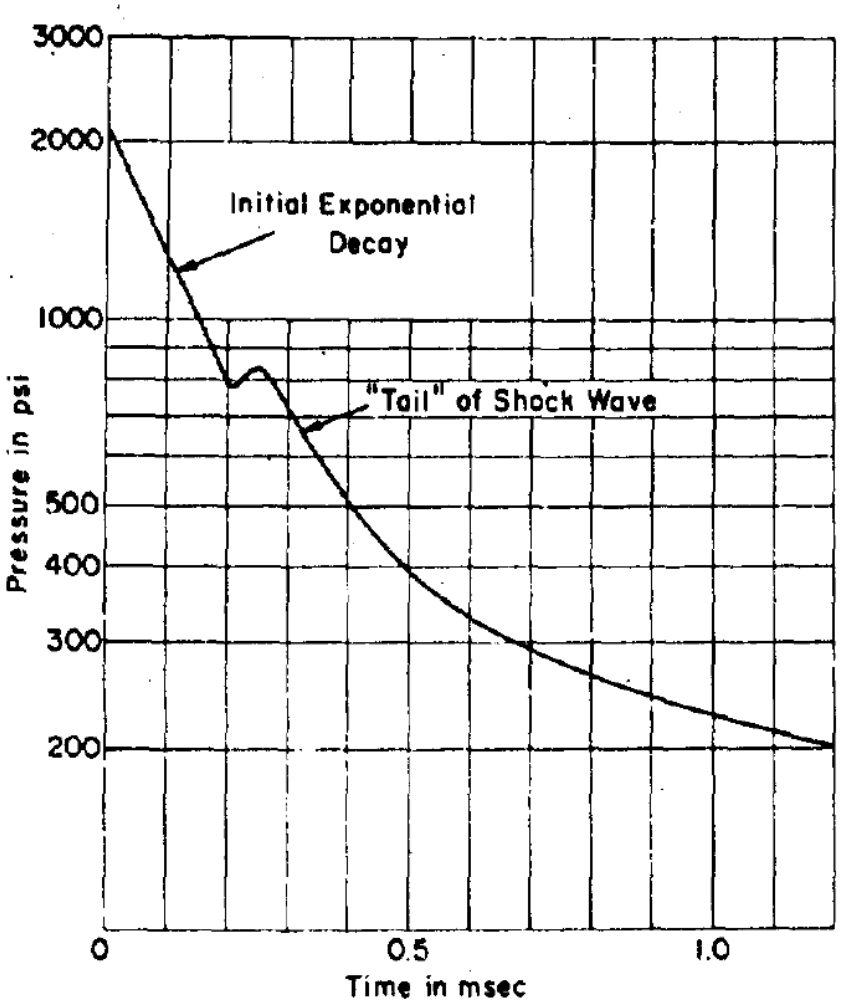

Fig. 2 Shock wave from 19-lb TNT at 20 ft

Figure 51. TNT shock wave at 20ft 19-lb charge. Source [4].

Table 3. Commonly used explosives and their respective detonation. velocities. Source [5].

EXPLOSIVE	*FORMULA*	*DENSITY (G/CC)*	*DET. VELOCITY (M/SEC)*
TNT	$C_7H_5N_3O_6$	1.60	6940
RDX	$C_3H_6N_6O_6$	1.57	8940
COMP B	RDX/TNT/WAX 59.4/39.6/1.0	1.68	7900
H-6	RDX/TNT/AL/WAX 45.1/29.2/21.0/4.7	1.74	7440
PBXN-103	AP/AL/PNC/MTN/RESOURCINOL/TEGDN 38.73/27.19/6.92/24.36/0.36/2.44	1.89	6130
HBX-1	RDX/TNT/AL/WAX	1.72	7310
HBX-3	PBX/TNT/AL/WAX 31/29/35/5	1.82	7310

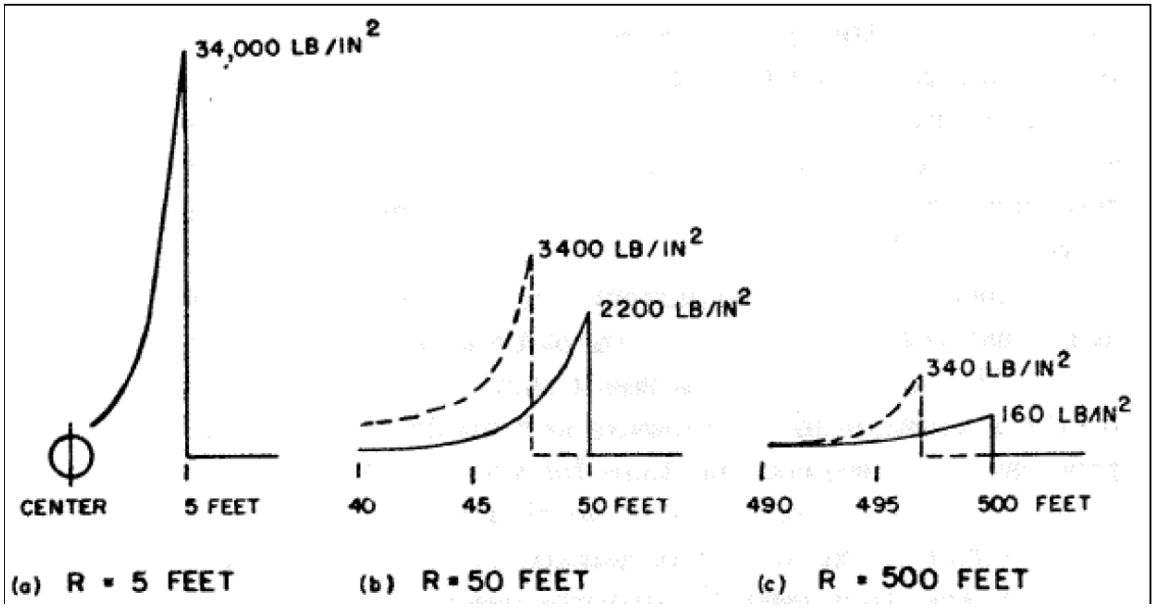

Figure 52. Shock wave pressure distribution of a 300 lbf TNT charge at three separate distances. Source [4].

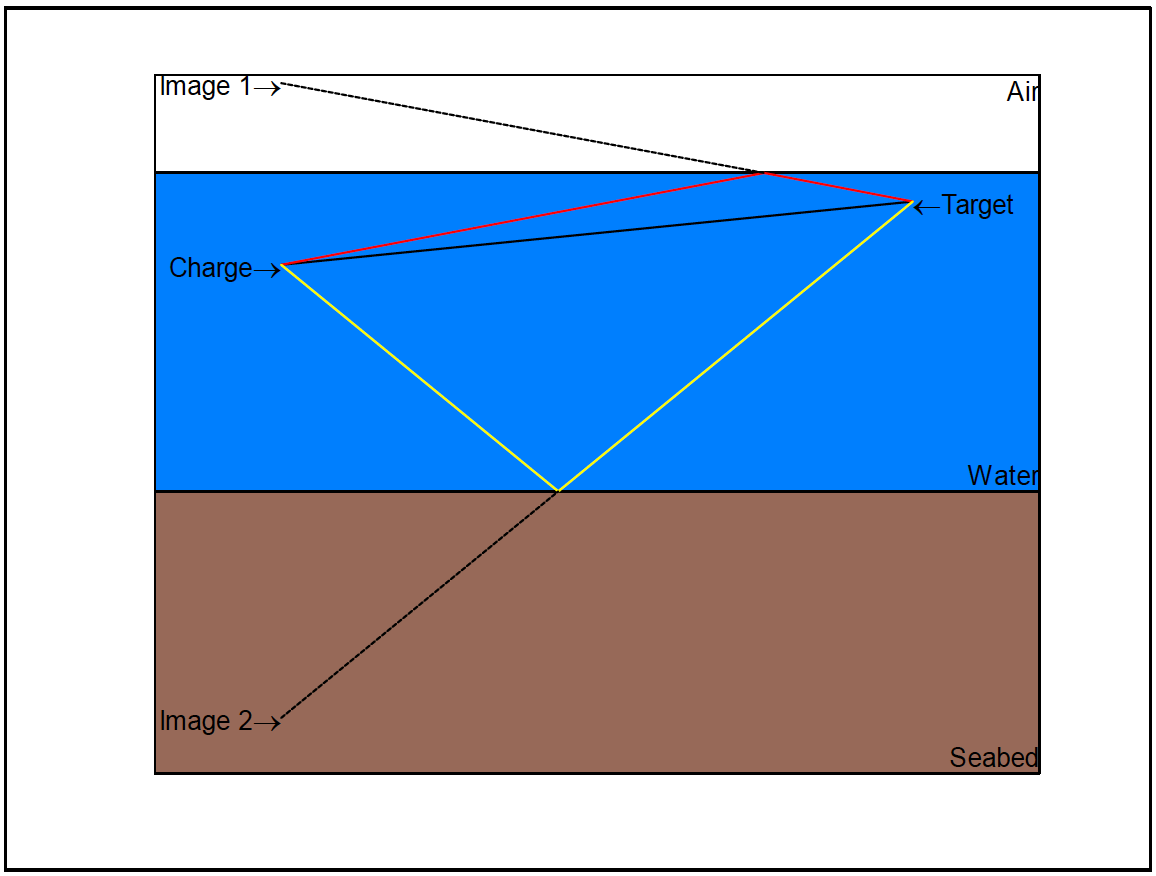

Figure 53. Underwater explosion geometry. Source [3].

Figure 54. Typical rupture profile of pressure vessel 1 view 1.

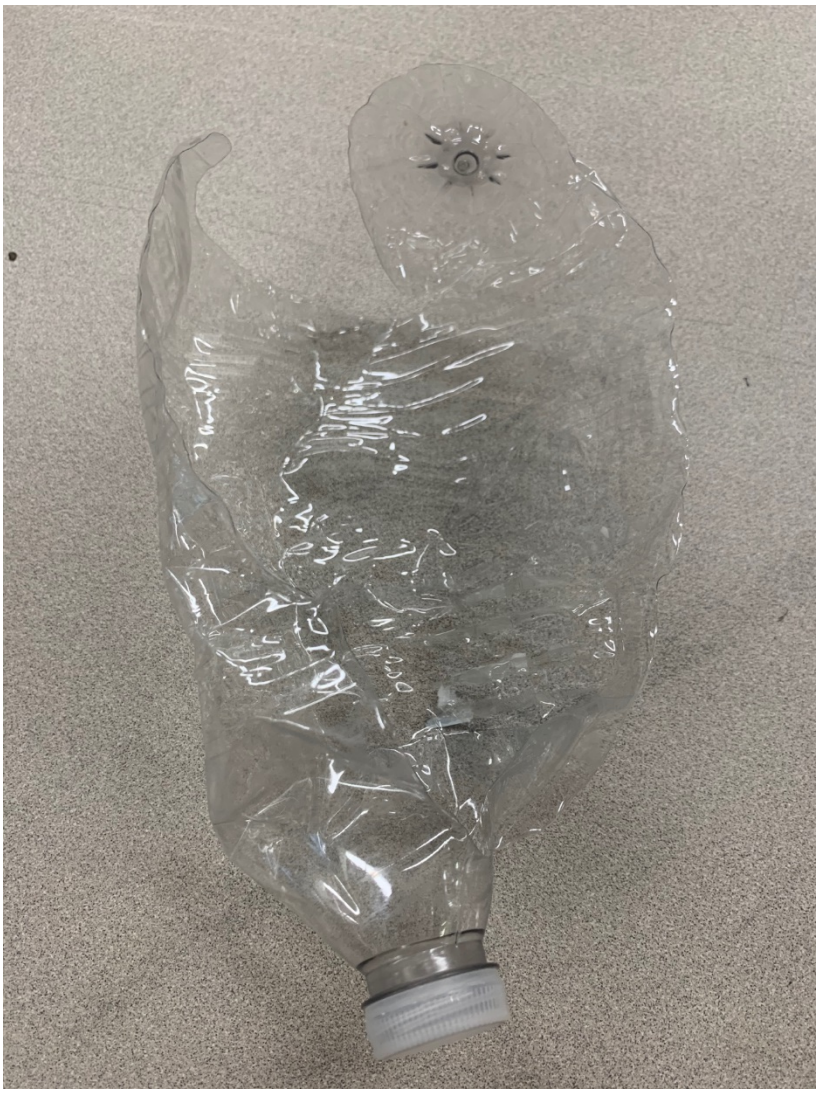

Figure 55. Typical rupture profile of pressure vessel 1 view 2.

THIS PAGE INTENTIONALLY LEFT BLANK

VI. CONCLUSIONS AND FUTURE WORK

PCB sent a regional technical representative to NPS to verify the experimental set up of their pressure sensor. Input signals were tested by switching the pressure sensor with a low noise microphone at a pre-determined decibel level. This sensor a PCB model number 378A04 was used to compare output signals with a known input signal using millivolts and decibels as appose to the pressure sensor using millivolts and pascals. This input was compared to the output of the testing equipment that was being used. The input and output signals matched exactly meaning that data acquisition was being performed correctly and in accordance with PCB's standards and recommendations. This helped to validate the results that were being seen specifically the negative pressure oscillations. Nothing on the NPS side of data collection or on the PCB side of data collection was being conducted incorrectly. This meant that the results that were being seen were not inaccurate or sometime of error or noise but actually occurring during underwater bubble pulses.

The main hypothesis for the negative pressure in the testing is that a vacuum is formed behind each peak pressure wave. A vacuum would read as a negative pressure in this type of testing. This vacuum and the rate at which it occurs would be critical in testing how damaging the shock bubble is during underwater explosion events. This vacuum has been unable to be accurately tested or measured in full-scale underwater explosion events because of the sever and damaging effects explosives have on testing equipment.

During this testing only one sensor was used. However, three additional sensors have since been ordered and have arrived at NPS. Being able to put sensors at all four corners of the tank would help test for reflective and refractive pressure wave properties. Four sensors in a row at equal distances would help to validate the Po curve created for dry ice and liquid nitrogen. Four sensors can also help test how the pressure wave develops above and below the pressure vessel as well as on either side of it. This would help to give justification to any FEA models designed and built for a certain ship or ship system.

Using a software such as Ansys to conduct a FEA model to show how this experiment validates a model and vice versa would help to close the loop between

modeling software and experimental design and lay groundwork for a procedure on how to use the tank for future thesis students and their research.

One of my ideas to relieve pressure on a ships keel from an underwater explosion that could be tested on a model in this tank would be an explosion door similar to that on a diesel engine crank case. This can be seen in Figure 5. Many ships are built with a double bottom hull design meaning there is a web of I-beams with spacing between them as seen in Figure 6. Sometimes this space is filled with fuel, ballast water (seawater) or nothing and is simply just filled with air and sealed off and only open for routine inspections. If an explosion door was able to be fitted to the hull plating it might be able to absorb some of the explosion force and dissipate it into the double bottom hull. This would in turn create less of an implosion or after shock lessening the likely hood of the ships keel to break or snap.

The double bottom hull of any ship or model could be tested experimentally or modeled to see where peak stresses and strain would occur. Once this place was found explosion doors could be fitted to the model and the double bottom tank void filled with a coating or Non-Newtonian fluid. Testing of these coatings or types of fluid and how much shock they help to absorb or dissipate could help in minimizing the damaging effects of underwater explosion events.

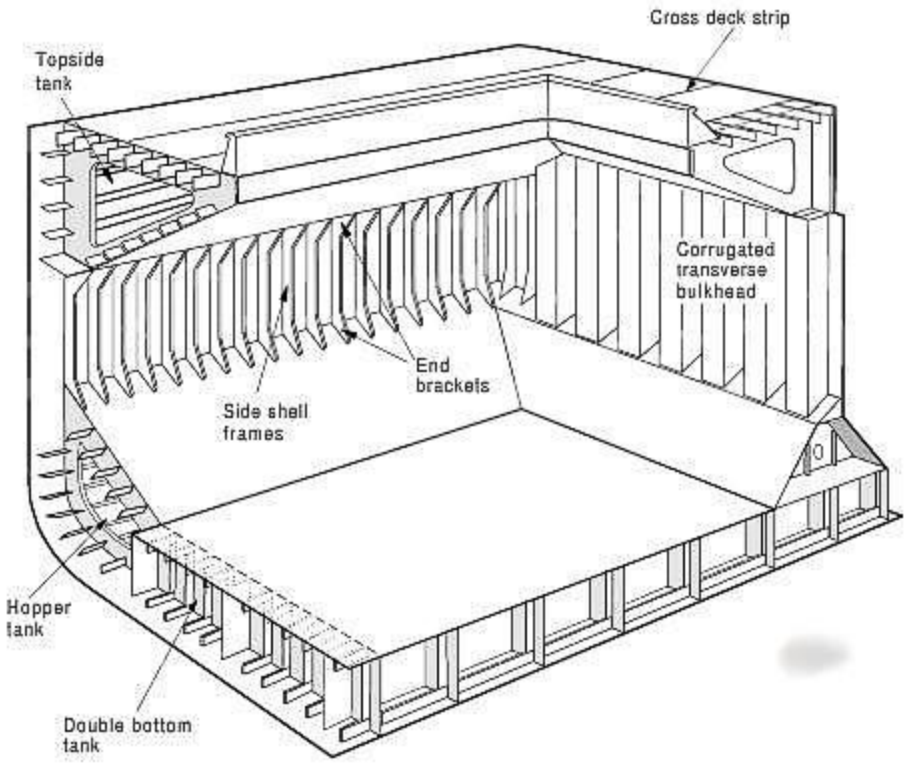

Figure 56. Typical ship double bottom hull design. Source [17].

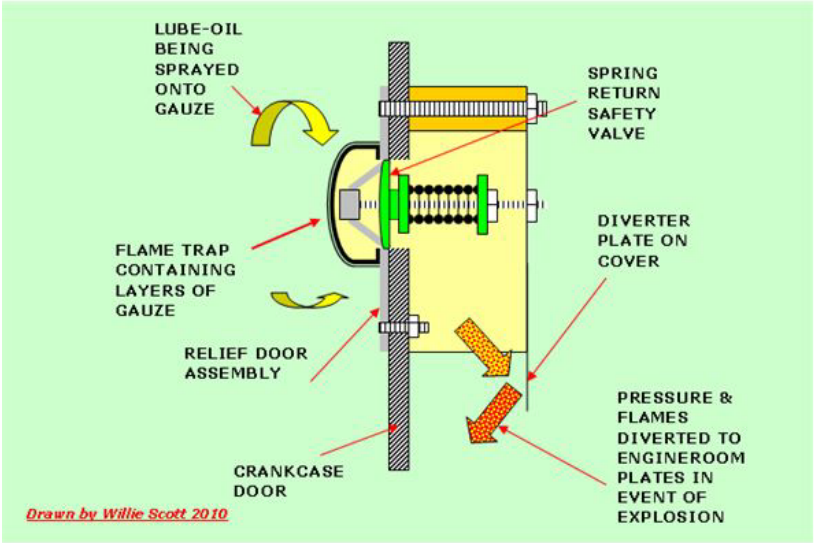

Figure 57. Diesel crank case explosion door. Source [18].

I would suggest that future students conduct the same tests but in much deeper water to validate that the tank is operating as it was designed to with minimizing wave reflection with its wooden sides.

For implosion-only testing it would also be of use to test in deeper water. This would cause a greater delta in pressure from inside the balloon to the surrounding water column. This might cause the sensor to pick up the pressure difference when the balloon collapses where in the tank it was unable to. The sensor could be placed in several places especially with the addition of three more new sensors for a total of four sensors. The main place that has not been tried before is the pressure sensor being inside of the balloon.

Placing a sensor inside of the balloon allows for a test that is impossible to be conducted with explosives to be performed. Watching how the sensor reacts to the collapsing of the water column into the balloon that was previous filled with air and onto the sensor will yield a result that could be worth analyzing further.

Further testing of coatings will be performed utilizing the testing method studied and analyzed here. A system installed and working at NPS that is capable of measuring both underwater pressure, time, and strain on an underwater member will help thesis students put new cutting-edge ideas to the test. Waterproof strain gauges can easily be added to this system and used in tandem during the same test cycle.

During this testing only one sensor was used. However, three additional sensors were since ordered and have arrived at NPS. Being able to put sensors at all four corners of the tank would help test for reflective and refractive pressure wave properties.

APPENDIX A. CALIBRATION CERTIFICATE

CALIBRATION CERTIFICATE

Model:	138A02
Serial #:	11204
Description:	Pressure Sensor
Type:	ICP
Sensitivity*:	4.878 mV/PSI 707.5 mV/MPa
Linearity*:	0.6% FS
Uncertainty:**	+/- 3 %
Bias:	10.03 VDC

Date: 1/7/2019
By: Jason Wojciechowski, Cal. Tech.
Station: 913 Dyn. High Pressure (Test Procedure AT601-8)

Temp: 68 deg F [20deg C]
Humidity: 35 %

Cert #: 731116

* Zero based, least-squares straight line.

** Measurement uncertainty represented using a coverage factor of k=2 which provides a level of confidence of approximately 95 %.

Condition of Unit:
As Found: Not applicable
As Left: In tolerance, new unit

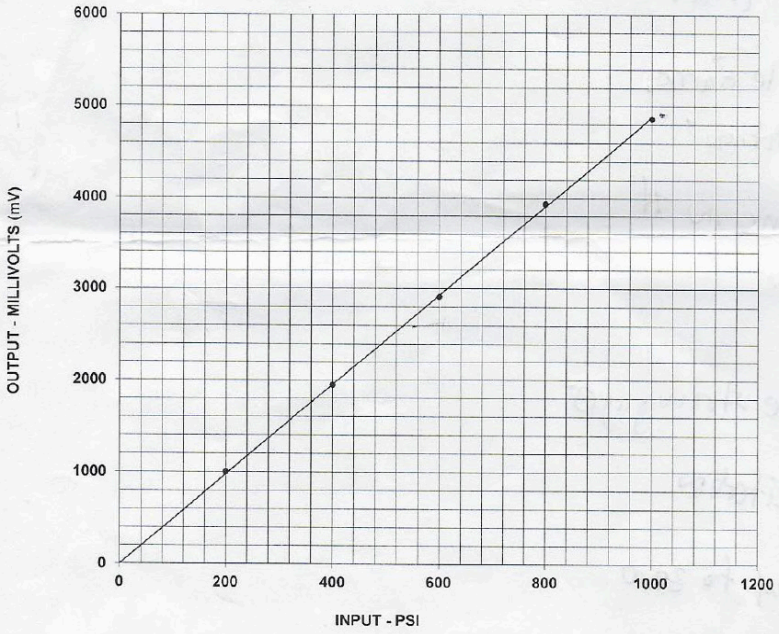

TEST DATA

INPUT (PSI)	OUTPUT (mV)
200	1002
400	1947
600	2911
800	3932
1000	4861

Notes:
1 Station #16
2 Calibration is traceable to NIST up to 15,000 psi static and is accredited to ISO 17025 and ANSI/NCSL Z540.3.
3 NIST traceability through PCB control # CA 1075.
4 This certificate may not be reproduced, except in full, without written approval from PCB Piezotronics, Inc.

ilac-MRA ACCREDITED
CALIBRATION CERT #1862.01

PCB PIEZOTRONICS INC.
Tel: 716-684-0001 Fax: 716-684-0987 Email: sales@pcb.com
3425 Walden Avenue, Depew NY 14043

Page 1 of 1

PCB PIEZOTRONICS
MTS SYSTEMS CORPORATION

CERTIFICATION OF CONFORMANCE

Title Page of Calibration Certificate Documentation

CUSTOMER:

Naval Postgrad School
Bldg 349
1988 Lake Delmonte
Monterey, CA 93943
UNITED STATES

PURCHASE ORDER #: 79780

PCB ORDER #: 421803

QTY	ITEM	DESCRIPTION
1	W138A02/-0013	PRESSURE SENSOR, W138A02/038CY010AC
		00011204

Notes:

1. This document certifies that the subject item(s) have been manufactured, repaired (if applicable), tested, or inspected in accordance with referenced purchase order and conform(s) to applicable specifications per PCB Quality Policy Manual Rev. M 10/03/2018.
2. Equipment used in validation is traceable to NIST and appropriate records are on file.
3. Calibrations comply with ISO 17025 and ANSI/NCSL Z540.3-2006 except as noted on associated calibration certificate(s). Order placement is an acknowledgement and acceptance of measurement capability. Product is compliant with specification if measured value is within or equal to the specification tolerance. Product is not compliant with specification if measured value falls outside the specification tolerance.
4. Calibrations are performed using processes having a test uncertainty ratio (TUR) of four or more times greater than the unit calibrated, unless otherwise noted on the calibration certificate. Calibration at 4:1 TUR provides reasonable confidence that the instrument is within product specifications.

APPENDIX B. DRY ICE MATLAB CODE

Table of Contents

Dry Ice Data

The following contains data collected from dry ice testing at various distances. The data is filtered, converted,
and plotted for data analysis purposes.

```
clear all
clc
```

Load Data

```
load 'dryice.mat'
```

Data Filtering

The following data sets contain dry ice explosions at 0 ft, 2 ft, 4 ft, 6 ft, and 8 ft.

```
V0ft1DI(1:2) = [];
V0ftDI(1:2) = [];
V2ft1DI(1:2) = [];
V2ft2DI(1:2) = [];
V2ftDI(1:2) = [];
V4ft1DI(1:2) = [];
V4ft2DI(1:2) = [];
V4ftDI(1:2) = [];
V6ftDI(1:2) = [];
V8ftDI(1:2) = [];
T0ft1DI(1:2) = [];
Time0ftDI(1:2) = [];
T2ft1DI(1:2) = [];
Time2ftDI(1:2) = [];
T2ftDI(1:2) = [];
T4ft1DI(1:2) = [];
T4ft2DI(1:2) = [];
T4ftDI(1:2) = [];
T6ftDI(1:2) = [];
T8ftDI(1:2) = [];
% The filtfilt function is used to filter the noise from the original
data
1
% Filter design
[b,a] = butter(8,0.01);
%First method
aa = filtfilt(b,a,V0ft1DI);
bb = filtfilt(b,a,V0ftDI);
c = filtfilt(b,a,V2ft1DI);
d = filtfilt(b,a,V2ft2DI);
e = filtfilt(b,a,V2ftDI);
f = filtfilt(b,a,V4ft1DI);
```

```
g = filtfilt(b,a,V4ft2DI);
h = filtfilt(b,a,V4ftDI);
i = filtfilt(b,a,V6ftDI);
j = filtfilt(b,a,V8ftDI);
```

Conversion

From mV to Pa

```
aa = aa/4.878*1000;
bb = bb/4.878*1000;
c = c/4.878*1000;
d = d/4.878*1000;
e = e/4.878*1000;
f = f/4.878*1000;
g= g/4.878*1000;
h = h/4.878*1000;
i = i/4.878*1000;
j = j/4.878*1000;
```

Plotting

```
figure (1)
plot(T0ft1DI,aa)
title('Dry iceat 0m Test 1')
xlabel('Time, [seconds]')
ylabel('Pressure, [Pa]')
axis([.5 1 -2.5 1])
grid on
figure (2)
plot(T2ft1DI,c)
title('Dry iceat 0.6m Test 3')
xlabel('Time, [seconds]')
ylabel('Pressure, [Pa]')
axis([.4 1 -2 1.5])
grid on
figure (3)
plot(T2ftDI,e)
title('Dry iceat 0.6m Test 2')
xlabel('Time, [seconds]')
2
ylabel('Pressure, [Pa]')
axis([.436 .56 -1.5 2.5])
grid on
figure (4)
plot(T4ft1DI,f)
title('Dry iceat 1.29m Test 3')
xlabel('Time, [seconds]')
ylabel('Pressure, [Pa]')
axis([.985 1.2 -4 4])
grid on
figure (5)
plot(T4ft2DI,g)
title('Dry iceat 1.29m Test 2')
xlabel('Time, [seconds]')
ylabel('Pressure, [Pa]')
axis([.812 1 -4.5 4])
grid on
```

```
figure (6)
plot(T4ftDI,h)
title('Dry iceat 1.29m Test 1')
xlabel('Time, [seconds]')
ylabel('Pressure, [Pa]')
axis([1.14 1.34 -2 1.5])
grid on
figure (7)
plot(T6ftDI,i)
title('Dry iceat 2m Test 1')
xlabel('Time, [seconds]')
ylabel('Pressure, [Pa]')
% axis([1.1925 1.34 -11 18])
grid on
figure (8)
plot(T8ftDI,j)
title('Dry iceat 2.44m Test 1')
xlabel('Time, [seconds]')
ylabel('Pressure, [Pa]')
axis([.36 .6 -3.4 3.5])
grid on
figure (9)
plot(Time0ftDI,bb)
title('Dry iceat 0.0m Test 2')
xlabel('Time, [seconds]')
ylabel('Pressure, [Pa]')
axis([.857 1 -11 20])
grid on
figure (10)
plot(Time2ftDI,d)
3
title('Dry iceat 0.6m Test 1')
xlabel('Time, [seconds]')
ylabel('Pressure, [Pa]')
axis([1.05 1.3 -5 7])
grid on
4
5
6
7
8
Published with MATLAB® R2017b
9
```

THIS PAGE INTENTIONALLY LEFT BLANK

APPENDIX C. LIQUID NITROGEN MATLAB CODE

Table of Contents

Liquid Nitrogen

The following contains data collected from liquid nitrogentesting at various distances. The data is filtered, converted, and plotted for data analysis purposes.

```
clear all
clc
```

Load Data

```
load 'liquidnitrogen.mat'
```

Data Filtering

The following data sets contain dry ice explosions at 0 ft, 2 ft, 4 ft, and 6 ft.

```
V2ft(1:2) = [];
V2ft1(1:2) = [];
V2ft2(1:2) = [];
V4ft(1:2) = [];
V4ft1(1:2) = [];
V6ft(1:2) = [];
V6ft1(1:2) = [];
T2ft(1:2) = [];
T2ft1(1:2) = [];
T2ft2(1:2) = [];
T4ft(1:2) = [];
T4ft1(1:2) = [];
T6ft(1:2) = [];
T6ft1(1:2) = [];
% The filter function was used to remove the noise from the original
data.
% There was significantly less noise observed in liquid nitrogen than
dry
% ice.
% Filter design
windowSize = 100;
b = (1/windowSize)*ones(1,windowSize);
a = 1;
1
% First method
yf1 = filter(b,a,V2ft);
yf2 = filter(b,a,V2ft1);
yf3 = filter(b,a,V2ft2);
yf4 = filter(b,a,V4ft);
yf5 = filter(b,a,V4ft1);
yf6 = filter(b,a,V6ft);
yf7 = filter(b,a,V6ft1);
```

Conversion

From mV to Pa

```
V2ft = yf1/4.878*1000;
V2ft1 = yf2/4.878*1000;
V2ft2 = yf3/4.878*1000;
V4ft = yf4/4.878*1000;
V4ft1 = yf5/4.878*1000;
V6ft = yf6/4.878*1000;
V6ft1 = yf7/4.878*1000;
```

17.5

```
figure (1)
plot(T2ft,V2ft)
title('Liquid nitrogen at 0.6m Test 1')
xlabel('Time, [seconds]')
ylabel('Pressure, [Pa]')
%axis([1.3 2 -5 10])
grid on
figure (2)
plot(T2ft1,V2ft1)
title('Liquid nitrogen at 0.6m Test 2')
xlabel('Time, [seconds]')
ylabel('Pressure, [Pa]')
axis([.57 1.5 -5 11])
grid on
figure (3)
plot(T2ft2,V2ft2)
title('Liquid nitrogen at 0.6m Test 3')
xlabel('Time, [seconds]')
ylabel('Pressure, [Pa]')
%axis([1.18 1.5 2.5 7])
grid on
figure (4)
plot(T4ft,V4ft)
title('Liquid nitrogen at 1.29m Test 1')
xlabel('Time, [seconds]')
ylabel('Pressure, [Pa]')
2
axis([.48 1.2 -4 5])
grid on
figure (5)
plot(T4ft1,V4ft1)
title('Liquid nitrogen at 1.29m Test 2')
xlabel('Time, [seconds]')
ylabel('Pressure, [Pa]')
axis([.78 1.8 -4 6])
grid on
figure (6)
plot(T6ft,V6ft)
title('Liquid nitrogen at 2m Test 1')
xlabel('Time, [seconds]')
ylabel('Pressure, [Pa]')
```

```
%axis([.2 1.1 -4 5])
grid on
figure (7)
plot(T6ft1,V6ft1)
title('Liquid Nitrogen at 2m Test 2')
xlabel('Time, [seconds]')
ylabel('Pressure, [Pa]')
%axis([.87 2 -3 5])
grid on
3
4
5
6
Published with MATLAB® R2017b
7
```

THIS PAGE INTENTIONALLY LEFT BLANK

LIST OF REFERENCES

[1] Kwon, Y., personal communication, 22 September 2018.

[2] Didoszak, J., personal communication, 23 June 2018

[3] Naval Sea Systems Command, 1989, "Military Specification: Shock Tests, H.I. (High-Impact) Shipboard Machinery, Equipment, and Systems," Naval Sea Systems Command, Washington, DC.

[4] Department of the Navy, 1987, "Shock Hardening of Surface Ships," OPNAVINST 9072.2.

[5] Snay, H. G., 1962, "Underwater Explosion Phenomena: The Parameters of Migrating Bubbles," Technical Report NAVORD 4185, U.S. Naval Ordnance Laboratory, White Oak, MD.

[6] Snay, H. G., 1962, "The Scaling of Underwater Explosion Phenomena," Naval Ordnance Lab, White Oak, MD.

[7] Cole, R. H., 1948, Underwater Explosions, Princeton Press, Princeton.

[8] Schultz, N., personal communication, 14 November 2019.

[9] Arons, A. B., and Yennie, D.R., 1948, "Energy Partition in Underwater Explosions Phenomena," Reviews of Modern Physics, 20(30), 519–536

[10] Arons, A. Yennie, D. and Cotter, T. J., "Long Range Shock Propagation in Underwater Explosion Phenomena II," in Underwater Explosion Research: Volume I – The Shock Wave, 1949, pp. 1473–1584.

[11] Prendergast, G. R., 2010, "Underwater Explosion Whipping Response of Monohull versus Trimaran Vessels," Ph.D. dissertation, Naval Postgraduate School, Monterey, CA.

[12] Naval Sea Systems Command, 1994, "Shock Design Criteria for Surface Ships," Naval Sea Systems Command, NAVSEA 0908-LP-000-3010A.

[13] Bangash, M, 1993, Impact and Explosion: Analysis and Design, CRC Press, Oxford.

[14] Ohara, G. J., 1965, "Background for Mechanical Shock Design of Ships Systems." Naval Research Laboratory, Washington, DC.

[15] "Jet Flows at Shallow Underwater Explosions." (n.d.). Hydrodynamics of Explosion High-Pressure Shock Compression of Condensed Matter, 297–358.

[16] Itoh, S. (2007). “The Industrial Applications of Underwater Shock Wave.” Explosion, Shock Wave and Hypervelocity Phenomena Materials Science Forum, 361-372.

[17] Haider, H. M. K, 2018, “Bulk Carrier Guide,” http://www.bulkcarrierguide.com.

[18] Clarke, F. E., 2009, “Crankcase Explosions in Marine Engines,” Journal of the American Society for Naval Engineers, 68(1), 122–128.

INITIAL DISTRIBUTION LIST

1. Defense Technical Information Center
   Ft. Belvoir, Virginia

2. Dudley Knox Library
   Naval Postgraduate School
   Monterey, California